Polymers for Hydrogen Infrastructure and Vehicle Fuel Systems:
Applications, Properties, and Gap Analysis

R. R. Barth, Sandia National Laboratories
K. L. Simmons, Pacific Northwest National Laboratory
C. San Marchi, Sandia National Laboratories

Sandia National Laboratories

Polymers for Hydrogen Infrastructure and Vehicle Fuel Systems:
Applications, Properties, and Gap Analysis

R. R. Barth
Sandia National Laboratories
P.O. Box 969, MS 9042
Livermore, CA 94551

K. L. Simmons
Pacific Northwest National Laboratory
P.O. Box 999, MSIN K2-44
Richland, WA 99352

C. San Marchi
Sandia National Laboratories
P.O. Box 969, MS 9161
Livermore, CA 94551

Abstract

This document addresses polymer materials for use in hydrogen service. Section 1 summarizes the applications of polymers in hydrogen infrastructure and vehicle fuel systems and identifies polymers used in these applications. Section 2 reviews the properties of polymer materials exposed to hydrogen and/or high-pressure environments, using information obtained from published, peer-reviewed literature. The effect of high pressure on physical and mechanical properties of polymers is emphasized in this section along with a summary of hydrogen transport through polymers. Section 3 identifies areas in which fuller characterization is needed in order to assess material suitability for hydrogen service.

ACKNOWLEDGMENTS

CONTENTS

FIGURES

TABLES

1 APPLICATIONS AND MATERIALS

The development of hydrogen fuel cell systems and the associated hydrogen distribution and dispensing infrastructure will require a multi-materials approach that utilizes the most effective combination of materials to achieve safe, cost-effective construction. This section seeks to identify the polymer materials that are exposed to gaseous hydrogen in evolving hydrogen energy applications, with particular emphasis on hydrogen fuel cell vehicles and their fueling infrastructure. For the vehicle application, gaseous hydrogen fuels are stored on-board at pressures as high as 70 MPa, while the fueling station compression/storage/dispensing system can be at significantly higher pressure, as high as 100 MPa. Ambient temperatures for both applications range from 233 K (−40°C) to 358 K (+85°C), except within compressors, where temperatures as high as 473 K (200°C) can be reached. For the purposes of this section, hydrogen energy technologies are broken down into (i) distribution and delivery, (ii) fueling stations, and (iii) vehicle fuel system. High-pressure gaseous systems are emphasized here, since high pressure is one of the dominant challenges associated with the current landscape of hydrogen fuels. Cryogenic distribution of gases in the liquid form (including hydrogen) is a mature technology and an important component of distribution of hydrogen fuels. While the use of polymers with cryogenic fluids is not a focus of this effort, a brief discussion of polymers in cryogenic hydrogen systems is provided at the end of this report. Additionally, the design and integration of hydrogen systems as well as discussion of competing materials and technologies (e.g., metals) are beyond the scope of this document.

1.1 Distribution and delivery

1.1.1 Piping and pipelines

There are over 1,000 km of hydrogen pipeline networks in North America and more than 1,500 km in western Europe. In the United States, most of these pipelines are located along the Gulf Coast to refineries and chemical manufacturing [1]. The Hydrogen Standardization Interim Report summarizes service data for hydrogen pipelines in the United States [2]. Existing pipelines are steel; however, there is growing interest in fiber-reinforced polymer (FRP) pipelines. FRP pipelines have the advantage that multiple, small-diameter lines can be installed together; the small diameter allows operation at higher pressure than large diameter pipelines and the multiple lines further increase the volume that can be transported [1].

The FRP piping and pipelines typically consist of an impermeable polymer liner with a fiber-reinforced overwrap of glass, Kevlar, basalt or even carbon fibers in an epoxy resin system [1]. The polymer liner materials have typically been high-density polyethylene (HDPE); this material is chosen for its excellent combination of low hydrogen permeability and low cost. Other polymer systems are also being considered, such as nylons, which display lower hydrogen permeability. The ASME B31.12 committee is actively considering FRP for hydrogen piping and pipelines. Current pipeline life expectancy is 20 years, although there is interest in extending design life to 50 years. The large capital investment associated with installing pipelines is a strong driver for longer design life [1].

1.1.2 Tube trailers and batch distribution

Both gaseous hydrogen and liquid hydrogen are delivered by commercial trucks. Technologies associated with delivery of liquefied gases (such as nitrogen, hydrogen and others) are well

developed. Seamless steel tube trailers can deliver gaseous hydrogen at pressure less than 30 MPa [1]. Steel pressure vessels with FRP overwrap (Type II vessels) are also used for delivery of high-pressure gases. Delivery of gaseous hydrogen at pressure greater than 30 MPa is being developed using composite pressure vessel structures; in particular, carbon fiber composite pressure vessels (Type IV with HDPE liners) are being developed for tube trailers at pressures up to 54 MPa [1].

1.2 Fueling stations

Hydrogen dispensing systems are typically designed for refueling on-board storage systems to pressure of 35 or 70 MPa. The delivery time for refueling passenger vehicles is targeted to be four minutes or less. Currently, the industry is considering adopting compressed natural gas components for hydrogen with some changes in material compatibility for balance of plant components that are subjected to a wide range of pressures, flows and temperatures. The temperature of the gas within the pressure vessels increases during fill reaching temperatures significantly above ambient. The gaseous hydrogen fuel must be pre-chilled to around 233 K (−40°C) to ensure compliance with the 358 K (+85°C) limit currently specified for on-board storage systems when filled on short time scales [3]. The wide range of temperature, steep temperature gradients and high flow rates creates challenges with reliability of the components in the dispensing system, including polymer materials in dispensing hoses.

Actuated seals as in regulators and valves commonly use "soft-seat" polymer materials. Fixed joints also use polymer materials, such as elastomer O-rings. Such sealing applications exist in stationary storage and dispensers as well as in the vehicle fuel system. Seals will often experience large temperature gradients during refueling, as well as the full environmental temperature range (233 to 358 K), which represents temperatures near the minimum and maximum use temperature of common polymer materials. Compressors also use polymer seals; compressor seals differ from other sealing applications as they experience higher temperature (~200°C).

1.3 Vehicle fuel system

The vehicle fuel system refers to on-board storage at high pressure as well as the low-pressure delivery of gas to the fuel cell. Although they are not a focus of this document, cryogenic (liquid hydrogen) storage systems are discussed briefly in Section 3.3.2; liquid hydrogen systems include low pressure systems operating below 1 MPa [4] as well as the so-called cryo-compressed systems that store hydrogen at much higher pressure (but lower pressure than gaseous storage systems). The fuel cell stack itself is not considered here.

The primary challenges with polymer materials in the vehicle fuel system are associated with large pressure gradients and thermal transients during refueling operations as well as during consumption of the fuel. Environmental conditions (ambient temperature, humidity, etc.) may also be important considerations in some cases.

Fuel tanks on board passenger vehicles typically use Type III and Type IV pressure vessels due to their gravimetric and volumetric efficiency. The fast filling of Type IV pressure vessels can approach adiabatic compression due to the low thermal conductivity of the polymer liner and composite. The temperature change within the tank depends on the rate of filling, the volume, the

thermal properties of the composite structure, and the design of the pressure vessel boss/nozzle [3, 5]. Temperature excursions are especially important for polymer liners; during filling, the high flow rates may result in local temperature variations at the liner, different from the bulk gas temperature, that potentially exceed the design temperature of the liner material. Polymer liners are typically HDPE, although nylons are also being considered. Proprietary surface treatments that reduce leak rates are believed to be used for many of the liner systems. In addition, multi-component, multilayered liner systems are being considered [6].

Other components within the fuel system (i.e., balance of plant) will also experience some temperature variation during refueling. Additional thermal transients will occur during consumption of the fuel and as a result of fluctuations in the ambient environment. For gaseous storage systems, these temperature cycles will also induce pressure cycles, generally of low amplitude. In general, sealing applications on vehicle fuel systems are similar to those in the fueling station and utilize similar materials.

1.4 Materials

Table 1.1 lists several components of hydrogen systems and examples of associated polymeric materials. Some components that may also contain polymeric elements, such as sensors and transducers, are not included.

Many polymer materials are associated with seals in connections, compression equipment, valves, etc. Sealing materials are typically elastomeric materials, which have a relatively narrow temperature range for standard operation. Teflon (PTFE) is a semicrystalline thermoplastic also used in sealing applications and has the advantage that it can be used over a much wider range of temperatures.

The materials listed represent polymers being considered for use and may not be fully suitable for the applications described. Components constructed from polymer materials are known to be subject to a variety of failure types in high-pressure hydrogen systems, such as rupture and blistering of O-rings due to high-pressure cycling (rapid gas decompression). Anecdotal information suggests that dispensing hoses may fail after as few as 100 filling cycles. Improved understanding of the physical processes associated with these failure modes will aid in developing and selecting materials better suited to operation in high-pressure hydrogen environments. Materials for hydrogen service will likely become more specialized as the technologies mature.

Table 1.1 Examples of polymer materials used in high-pressure hydrogen infrastructure

Component	Description	Example materials[a]
Compressed hydrogen pressure vessels	Type III	Metallic liner; composite vessel: glass fiber or carbon fiber, epoxy resin
	Type IV	Polymer liner: HDPE, nylon; composite vessel: glass fiber or carbon fiber, epoxy resin
Pipelines	Multi-layer construction for high-pressure distribution (>10 MPa)	Polymer liner: HDPE, nylon; composite vessel: glass fiber or carbon fiber, epoxy resin
Piping, tubing	Monolithic construction for low-pressure distribution (<10 MPa)	HDPE, PP, PVC, CPVC
Mechanical compressors	Seals and coatings	Teflon composite, PEEK
Dispensing hoses		Proprietary/unknown material
Flange connections (low pressure)	O-rings, gaskets	Nitrile rubber, Viton, Teflon
Threaded connectors (high pressure)	O-rings	Nitrile rubber, Viton
Valves (manual, actuated, check, velocity, relief devices)	Pistons	PEEK
	O-rings, fittings, etc.	Nitrile rubber, Viton, Teflon
	Seals and gaskets	Teflon, Viton, nitrile rubber, EPM, fluorosilicone, silicone, Neoprene, Nylon, PEEK
	Valve seats	Nylatron, Vespel, PCTFE, Teflon

[a]Materials are defined in Section 2.

2 EFFECTS OF HIGH PRESSURE AND HYDROGEN ON MATERIAL PROPERTIES

2.1 Introduction

This section describes the influence of high pressure and hydrogen on the properties of polymers identified as applicable to hydrogen infrastructure and vehicle fuel systems. The information presented is compiled from peer-reviewed, published data available in the open literature. Some information on temperature effects is provided, but in general, the influence of temperature on material properties is covered extensively in many polymer textbooks and property handbooks and is not our focus here. Instead, we focus on identifying changes in polymer properties that result from exposure to high pressure, hydrogen, or both. This information is much more specialized to hydrogen infrastructure applications and is less often reported in standard works.

This document emphasizes the fundamental characterization of polymer materials, not of components such as seals, pipes, or pressure vessel liners. Also, although we consider the polymer constituents of composite materials (e.g., FRP) to be within our purview, it is not our purpose to review the properties of composite materials designed for specific applications. (We have, however, included references to studies of such systems when we have encountered them.) Rather, the purpose of this document is to provide information about the current state of knowledge of polymer properties in hydrogen and/or at high pressure. For readers interested in materials selection and system design, the references cited in this document should provide a good starting point for investigating the properties of materials of interest.

2.1.1 Differences between metals and polymers in the context of hydrogen compatibility

There are many differences between metals and polymers. The following brief summary highlights some of the most important differences relevant to hydrogen applications and is not intended to be comprehensive.

The properties of polymers depend not only on their chemical structure, by which they are typically designated, but on a variety of other factors. The most important of these are molecular weight (and molecular weight distribution) of polymer chains, and processing history. For example, the degree of crystallinity of a polymer is affected by the rate at which it is cooled from the molten state. Processing techniques like extrusion can induce orientation and extension of polymer chains, influencing properties. Fillers, plasticizers, crosslinking agents, and other additives are often incorporated to modify properties. Thus tremendous variety may be associated with a single polymer.

The effects of viscoelasticity govern much of polymer behavior. In practice, this means that polymer properties tend to be highly sensitive to test conditions such as temperature and rate of testing. (In metals, this is not generally true, although the presence of hydrogen may *induce* temperature and/or rate dependencies in metals.) Unlike metals, polymer properties are affected by hydrostatic pressure.

Polymers are not subject to hydrogen embrittlement in the same ways as metals. Hydrogen absorbed by polymers exists as a diatomic molecule; it does not dissociate as it is known to do in metals. The fact that it remains chemically intact does not necessarily imply that hydrogen does

not influence polymer properties. Some gases, notably carbon dioxide, become strong solvents for many polymers at high pressure and have a plasticizing effect on properties (i.e., the materials become significantly softer) [7]. Hydrogen is expected to be inert in the presence of most polymers, but its effects have rarely been explored at high pressures.

2.1.2 Classes of materials

We have divided the polymers of interest into four classes based on their microstructure. The first two of these are thermoplastics, and the second two are crosslinked into networks via a curing treatment.

2.1.2.1 Semicrystalline thermoplastics

Semicrystalline thermoplastics have both a crystalline (ordered) phase consisting of aligned chains packed into lamellae, and an amorphous (disordered) phase. The crystalline phase enhances the strength of the polymer. The approximate crystalline fraction, α, may range from very low proportions to about 70% by mass, depending on the polymer, molecular weight and thermomechanical history of the material. The density ρ of a particular polymer (given in units of g/cm^3) also provides an indication of crystalline fraction because the different phases have well-defined densities, with the crystalline phase having higher density. The quantities α and ρ for particular materials, when reported in this document, have been determined by the researchers and we have not made any independent effort to verify them. The semicrystalline polymers considered in this section are listed in Table 2.1. PP is included because it has potential applications in low-pressure piping; it is not thought to be of use in high-pressure applications.

Table 2.1 Material designations for semicrystalline thermoplastics[a]

Chemical name	Abbreviation	Trade name(s)
High density polyethylene	HDPE	

Polyamide (nylon)
    Polyamide 6/Polyamide 11
	PA
	    PA6/PA11
		Rilsan (PA11), Nylatron[b]

Polychlorotrifluoroethylene	PCTFE	Kel-F
Polyetheretherketone	PEEK	
Polyimide from pyromellitic dianhydride and 4,4′ diamino diphenyl ether		Vespel[c]
Polypropylene	PP	
Polytetrafluoroethylene	PTFE	Teflon

[a]Abbreviations from ASTM D1600, Standard Terminology for Abbreviated Terms Relating to Plastics.
[b]Nylatron is a family of nylon plastics typically filled with molybdenum disulfide powder.
[c]Vespel may be unfilled or may contain fillers such as PTFE, graphite, carbon fiber, or molybdenum disulfide.

Table 2.2 Material designations for amorphous thermoplastics[a]

Chemical name	Abbreviation	Trade name(s)
Chlorinated poly(vinyl chloride)	CPVC	
Poly(vinyl chloride)	PVC	

[a]Abbreviations from ASTM D1600, Standard Terminology for Abbreviated Terms Relating to Plastics.

Table 2.3 Material designations for elastomers[a]

Abbreviation	Description	Trade name(s)
BR	Polybutadiene	
CR	Polychloroprene	Neoprene
EPDM	Terpolymer of ethylene, propylene, and a diene with the residual unsaturated portion of the diene in the side chain	
EPM	Copolymer of ethylene and propylene	
FKM	Fluoroelastomers of vinylidene fluoride and one or more of: hexafluoropropylene, tetrafluoroethylene, fluorinated vinyl ethers, propylene, ethylene	Viton, Tecnoflon
FMQ, FVMQ	Silicone rubbers having fluorine substituent groups on the polymer chain (fluorosilicone rubber)	
HNBR	Hydrogenated poly(butadiene-*co*-acrylonitrile)	
IIR	Poly(isobutylene-*co*-isoprene) (butyl rubber)	
MQ, VMQ, PVMQ	Silicone rubbers with varying substituents on the polymer chain (P = phenyl, V = vinyl, M = methyl). Poly(dimethyl siloxane) (PDMS) is one type of MQ	Silastic
NBR	Poly(butadiene-*co*-acrylonitrile) (nitrile rubber)	Buna N, Perbunan

[a]Abbreviations and definitions from ASTM D1418, Standard Practice for Rubber and Rubber Latices—Nomenclature.

Table 2.4 Material designations for epoxies

Abbreviation	Description	Trade name(s)
DGEBA	Bisphenol A diglycidyl ether, also called Epichlorohydrin-bisphenol-A or epoxy resin	DER, EPON

2.1.2.2   Fully amorphous thermoplastics

Fully amorphous materials have a single disordered phase. Few amorphous materials have applications in hydrogen infrastructure. However, we consider PVC and CPVC (Table 2.2) to have potential applications in low-pressure hydrogen piping. PVC is commonly plasticized, usually with phthalate esters.

2.1.2.3   Elastomers

Elastomers are highly extensible, rubbery materials with the ability to recover elastically after stretching. They have excellent sealing properties. Some elastomers have some degree of crystallinity. Commercial preparations often contain filler particles such as carbon black. The elastomers considered in this document are given in Table 2.3. In this document we consider crosslinked (cured) versions of these materials only.

2.1.2.4   Epoxies

Epoxies are chemically crosslinked, rigid materials. They are most commonly prepared from a liquid epoxy resin, also known as bisphenol A diglycidyl ether (DGEBA) (Table 2.4). The epoxy resin is cured in the presence of a curing agent, often at elevated temperature. Epoxy resin systems also commonly use reactive diluents, such as butyl glycidyl ether, in small percentages for viscosity control. Epoxies prepared using any curing agent were considered to be within the scope of this document.

2.2 Physical properties

In hydrogen infrastructure and vehicle fuel system applications, temperatures range from −40°C to approximately 200°C. The highest temperatures are attained in compressors. In this section some of the general thermal characteristics of polymers are described very broadly and related conceptually to physical properties. The glass transition affects the amorphous fraction of polymers throughout the relevant temperature range. Polymer melting, softening and thermal stability are of importance at higher temperatures.

The effect of temperature on polymer behavior is discussed and documented extensively elsewhere. Numerous resources are available, so we have not attempted to reproduce this information in detail here. Additional general information on relationships between temperature and polymer physical properties is available in polymer textbooks (e.g., Ref. [8]). Parameters such as glass transition temperature, melting temperature, operating temperature range and so forth are given in reference handbooks and in manufacturer documentation.

2.2.1 Glass transition temperature

The glass transition is an important property that provides a basis for understanding polymer behavior. It is a reversible physical change in amorphous materials that is related to the concept of free volume (the unoccupied space between polymer chains) and the consequent mobility of polymer chain segments. At temperatures below this transition, the free volume is low and the amorphous fraction is glassy and rigid; at temperatures above this transition, chain segments have greater mobility and the material behaves in a rubbery, more ductile fashion. The glass transition temperature T_g is taken as the midpoint of the temperature range over which the transition occurs. Properties undergoing relatively abrupt changes at the glass transition include

shear modulus or modulus of elasticity, coefficient of thermal expansion and heat capacity, any of which may be used to characterize T_g experimentally.

Plasticization, that is, reduction of T_g, occurs when a material of low molecular mass is blended with the polymer. This is very commonly done with PVC to improve its flexibility.

Hydrostatic pressure compresses the amorphous phase of polymers, shifting the glass transition temperature to higher values. Increases in T_g of 15˚C over a pressure increase of 100 MPa are not unusual and these increases are often linear with hydrostatic pressure. As a rough point of reference, values of T_g for selected polymers are listed in Table 2.5. These are compiled from secondary sources (literature reviews and polymer reference books). Literature values of T_g for a given polymer can vary widely. We caution that the values given here must be considered ballpark figures, because T_g may be affected considerably by molecular weight, polymer history (including cure conditions), the technique used to characterize the glass transition, and heating/cooling rate. These values are reported in order to provide context for some of the pressure-induced increases in T_g reported by Jones Parry and Tabor [9], also given in Table 2.5.

When designing for hydrogen systems, the operating temperature and pressure ranges must be considered. This is particularly true for elastomers, which derive their important properties from their rubbery character. Elastomers become brittle and make poor seals below T_g. If the pressure increases T_g for a particular O-ring material, such that the material becomes rigid within range of

Table 2.5 Glass transition temperatures and increases in glass transition temperature with hydrostatic pressure

Material	T_g (˚C)	T_g increase per 100 MPa[a] (˚C)	Ref.
Semicrystalline thermoplastics			
HDPE	−110		[10]
PA6	64	16	[9]
PCTFE	100		[11]
PEEK	150		[11]
PP	−10		[11]
PTFE	115		[11]
Amorphous thermoplastics			
CPVC	135		[11]
PVC	75	13−19	[9]
PVC + 20% dioctyl phthalate	40	13−17	[9]
Elastomers			
Fluorosilicone rubber	−50	16	[10]
NBR	−28		[12]
Neoprene	−40		[11]
Silicone rubber	−50	16	[9]
Viton	−20		[12]

[a]Compiled in Ref. [9].

the minimum operating temperature, that elastomeric material is likely to perform poorly as an O-ring sealing material.

2.2.2 Melting, softening and thermal stability

Melting occurs in crystalline materials. In semicrystalline polymers, the melting temperature T_m refers to the temperature at which the crystalline (solid) fraction becomes amorphous (liquid) via a first-order phase transition. Many commonly used thermoplastics melt below 200°C, but PEEK and a number of fluoropolymers have melting temperatures greater than 200°C, making them appropriate for use in high-temperature compressor environments.

The melting temperature of polymers is expected to increase with hydrostatic pressure. HDPE has been extensively studied in this regard; T_m is about 130°C at atmospheric pressure but increases by about 20°C at 100 MPa [13]. T_m for PCTFE has been found to increase by 65°C per 100 MPa from its atmospheric value of 215°C [14].

Although polymer amorphous fractions do not melt, above T_g they are subject to gradual reductions in strength and viscosity with increasing temperature, and at sufficiently high temperature they soften and flow over relatively short timescales. Therefore, an arbitrary but strictly defined "softening point" is sometimes used to characterize a material in lieu of, or in addition to, a melting point. Two commonly used softening point measures are the Vicat softening temperature (specified in ASTM D1525) and heat deflection temperature (specified in ASTM D648). The Vicat softening temperature is the temperature at which a flat circular probe of 1 mm^2 cross-sectional area will penetrate a specimen to a depth of 1 mm. The heat deflection temperature is the temperature at which a standard test specimen deflects by a specified amount.

Crosslinked polymers (thermosets) decompose rather than flow at high temperatures. Although the decomposition temperature for many elastomers, as measured by thermogravimetric analysis, may be in the vicinity of 300−400°C, substantial degradation can occur over time at much lower temperatures. For most elastomers, recommended prolonged use operating temperatures are well below 200°C. In general, the thermal stability of fluoroelastomers is greater than for conventional hydrocarbon elastomers, and some may be suitable for continuous working temperatures of 200°C. Perfluoroelastomers (FFKM) such as Kalrez have very high thermal stability and are stable at continuous operating temperatures well above 200°C.

2.3 Mechanical properties

In the published literature there is relatively little data characterizing the mechanical properties of polymers in the presence of both hydrogen and high pressure (up to 100 MPa). Therefore, this section discusses the effects of high pressure and hydrogen separately.

There is large body of literature characterizing the mechanical behavior of polymers under high hydrostatic pressure. The bulk of the data consists of stress-strain measurements under tension, compression or torsion within an enclosed pressure chamber, most commonly using an incompressible (or nearly incompressible) liquid as the pressurizing medium. Most of these experiments were conducted on thermoplastics, usually amorphous thermoplastics, during the 1960s-1980s. The information they provide is a useful basis for understanding the influence of high pressure on polymer properties. Although these researchers did address some aspects of failure behavior of the materials, they focused on the comparatively dramatic effects of imposed

hydrostatic pressure on material strength and modulus of elasticity. The influence of pressure on various types of failure or material durability is much less explored in the scientific literature.

A number of researchers have studied the influence of high pressure on the mechanical properties of composites. These include glass reinforced plastic (GRP) [15-22], carbon fiber reinforced plastic (CFRP) [23, 24], PVC with glass fibers [25], and rubber modified epoxies [26]. Hoppel et al. [27] have reviewed the influence of high hydrostatic pressure on the mechanical behavior of composite materials.

The mechanical behavior of polymers in hydrogen environments, let alone at high pressure, is far less studied. A French group [28] has developed a device capable of performing mechanical tests in hydrogen environments up to 40 MPa and applied this equipment for the study of polymers. While other groups have similar equipment, most materials testing in gaseous hydrogen has been devoted to testing metals.

2.3.1 Tension, compression and shear behavior at high hydrostatic pressure

Polymers can exhibit brittle fracture at low extensions, but many are ductile under proper temperature and rate conditions and can support large deformations before failing. Thermoplastics often deform by yielding. Elastomers are capable of deforming to high extensions (several hundred percent strain) and recovering completely or nearly completely to their initial dimensions upon release. Very highly extended elastomers may exhibit yielding as well. In polymers, yielding behavior is characterized by a maximum in the engineering stress-strain curve, often called the yield point. Beyond this point, many polymers exhibit necking (local reduction in cross sectional area) followed by significant elongation of the neck region prior to failure.

Deformation, yield and failure have been characterized for a variety of polymers subjected to hydrostatic pressures up to hundreds of MPa, and occasionally greater than 1000 MPa. Tsirule and Tyunina [29] and Sauer [30] provide good overviews of this work. For many thermoplastic materials, the tensile strength and shear and elastic moduli are known to increase with hydrostatic pressure, often on the order of 50-100% per 100 MPa. We emphasize that this increase is due to the applied hydrostatic compression and does not have permanent effects on the material. For example, HDPE specimens pressurized to 1100 MPa and subsequently tested at atmospheric pressure have been found to exhibit the same deformation characteristics as never-pressurized specimens [31].

2.3.1.1 Tensile properties

Tensile properties are reported according to definitions in ASTM specification D638 for plastics, and in ASTM D412 for elastomers. The following nomenclature is used to summarize the tensile data:

Tensile strength (MPa)	Maximum load divided by the original cross-sectional area (may occur either at a yield point or at specimen break)
Elongation at max stress (%)	Engineering strain at the maximum load
Modulus of elasticity (MPa)	Ratio of stress to strain at the initial linear portion of the stress-strain curve

Relevant tensile data at various pressures are summarized for semicrystalline polymers in Table 2.6, for elastomers in Table 2.7, and for epoxy in Table 2.8. To illustrate trends, pressures greater than 100 MPa are included when available. Test temperature was room temperature, uncontrolled, unless otherwise indicated. Generally the dimensions of the test specimens used were much shorter than those recommended in the ASTM specifications, by as much as a factor of five. This is attributed to space limitations in the pressure chambers used for high-pressure experiments.

Tensile stress-strain properties of PP [32, 33] and PVC [34] under high pressure are also available and generally follow similar trends, but these data have not been included because we consider these materials relevant for low-pressure applications only.

Effect of pressure on tensile strength and modulus of elasticity

For a number of semicrystalline thermoplastics and elastomers, it has been reported that both tensile strength and modulus of elasticity increase approximately linearly with hydrostatic pressure. The general trend of an increase in these properties with pressure appears to be universal, although the linearity of the behavior does not. The increases have usually been attributed directly to increases in T_g. Compression reduces the mobility of the polymer chains in the amorphous phase, stiffening the material. Occasionally changes in tensile strength have been attributed to crystalline phase changes. For example, PTFE is thought to undergo a transformation from a hexagonal to triclinic structure in the vicinity of 30 MPa [35].

Effect of pressure on ultimate elongation

In general, the pressure dependence of the elongation at failure cannot be characterized in a straightforward fashion. In epoxies, no systematic variation in nominal failure strain with pressure has been found, although specimens exposed directly to the pressurizing medium consistently failed at lower strains [36].

Elastomers were rarely tested to failure in a high-pressure environment due to the high extensibility of the materials and low availability of space inside the pressure chambers. However, Pai et al. [12] developed a special pressure chamber allowing long extensions and reported the combined effect of pressure and temperature on the ultimate elongation of elastomers, which depended highly on the identity of the polymer. The variation in ultimate elongation over a 100 MPa pressure increase was on the order of 100-200%. Increases with pressure were observed for EPDM, silicone rubber, and Viton at room temperature; IIR and NBR showed maxima in ultimate elongation as a function of pressure at room temperature. The variations in behavior were attributed to differences in crystallinity and glass transition temperatures.

In semicrystalline materials, pressurization appears to decrease the nominal strain at break. For example, Vroom and Westover found that pressurization reduced the elongation at break for PCTFE tested in mercury [37]. Increasing pressure increased the strength of the material while decreasing its ultimate elongation [35, 37].

The mechanisms for pressure-induced changes in elongation at break are not well understood, and the effects of compression on failure are complex. Cavitation and crazing, two phenomena often associated with tensile fracture, are volume-increasing processes likely to be inhibited by high hydrostatic pressure. This has been illustrated via experiments with highly drawn polyethylene samples: at atmospheric pressure, highly drawn polyethylene becomes opaque from

Table 2.6 Tensile properties of semicrystalline thermoplastics under hydrostatic pressure

Material	Description	Strain rate (min^{-1})	Pressure medium	Pressure (MPa)	Tensile strength[a] (MPa)	Elongation at max stress (%)	Modulus of elasticity (MPa)	Ref.
HDPE	ρ=0.946	0.20	kerosene	0.1	26.1	14	1200	[32]
				69	—	—	1800	
				140	40	12	2400	
				210	48	—	3000	
				280	52	5.4	3200	
	ρ=0.950	0.04	castor oil + 20% methanol	0.1	25	15	1100	[31]
				140	34	14	2000	
				280	55	9.2	2700	
	ρ=0.96	0.30 0.14	castor oil	0.1	32	—	—	[38]
				770	92			
PCTFE	—	—	—	0.1	37	—	—	[30]
				140	61	—	—	
				280	87	—	—	
				410	110[b]	—	—	
				690	130[b]	—	—	
	—	0.2	mercury	0.1	38	1.3	—	[37]
				34	46	1.5	—	
				69	54	1.6	—	
				100	60	1.6	—	
				140	68	1.7	—	
				170	75	1.7	—	
				210	82	1.8	—	
PTFE	—	2	mercury	0.1	31[b]	220	—	[37]
				34	35[b]	140	—	
				69	40[b]	100	—	
				100	50[b]	81	—	
				140	54[b]	76	—	
				170	55[b]	59	—	
				210	60[b]	60	—	
	—	0.20	kerosene	0.1	17[b]	130	—	[39]
				210	47[b]	60	—	
				410	62[b]	27	—	
	Halon G-80 ρ=2.17 α~57%	0.26	water	0.1	13.6	80	—	[35]
				280	61.7[b]	110	—	
				550	79.7[b]	65	—	
				830	96.5[b]	63	—	

[a]Strength at yield unless otherwise indicated.
[b]Tensile strength at break.

19

Table 2.7 Tensile properties of elastomers under hydrostatic pressure

Material	Description	Strain rate (min^{-1})	Pressure medium	Pressure (MPa)	Tensile strength[a] (MPa)	Elongation at max stress (%)	Modulus of elasticity (MPa)	Ref.
CR	—	0.7	petroleum ether	0.1 100 200	— — —	— — —	5.8 10 55	[40]
EPDM	—	1.65	glycerol	0.1 35 69 170	14 24 26 31	— — — —	— — — —	[12]
Fluoro-silicone	Silastic LS 53	0.3	petroleum ether	0.1 100 200	— — —	— — —	5.0 5.6 6.6	[40]
IIR	—	1.65	glycerol	0.1 34 64 140 200	18 21 22 23 24	— — — — —	— — — — —	[12]
NBR	—	1.65	glycerol	0.1 31 64 140 200	13 24 27 31 30	— — — — —	— — — — —	[12]
NBR	Low nitrile content	0.3	petroleum ether	0.1 100 200	— — —	— — —	8.9 11 16	[40]
Silicone	—	1.65	glycerol	0.1 30 60 130	7.4 10 11 11	— — — —	— — — —	[12]
Viton	—	1.65	glycerol	0.1 32 64 140 200	11 16 22 26 31	— — — — —	— — — — —	[12]
Viton	—	0.3	petroleum ether	0.1 100 200	— — —	— — —	6.3 11 630	[40]

[a]Strength at yield unless otherwise indicated.

Table 2.8 Tensile properties of epoxies under hydrostatic pressure

Material	Description	Strain rate (min^{-1})	Pressure medium	Pressure (MPa)	Tensile strength[a] (MPa)	Elongation at max stress (%)	Modulus of elasticity (MPa)	Ref.
DGEBA	Plasticized with dibutyl phthalate, cured with phthalic anhydride	0.0005	Plexol (a synthetic diester)	0.1	50	—	—	[36]
				25	53	—	—	
				50	58	—	—	
				75	68	—	—	
				100	72	—	—	
				150	74	—	—	
				200	89	—	—	
				250	92	—	—	
				300	97	—	—	

[a]Strength at yield unless otherwise indicated.

voids produced by cavitation, but polyethylene drawn to the same extension under high pressure is transparent due to a lack of voids [12]. However, tensile fracture in many materials has been observed to occur at lower strains with increasing pressure. Interactions with the pressurizing medium also appear to affect the ultimate elongation of the material.

Effect of pressurizing medium

Almost all experiments were performed ignoring possible effects of the pressurizing fluid. The pressure medium generally was found not to influence the stress and strain at yield. Exposure to the pressure medium tended to reduce the elongation to break, however, indicating that many pressure media could contribute to material failure. Specimens coated with rubber or wrapped with PTFE tape to prevent exposure to the pressure medium fractured at greater elongations than specimens exposed directly to the pressure medium [36, 41, 42].

Certain pressure media appear to soften some polymers. Vroom and Westover [37] found that many oils have a plasticizing effect on polymers (artificially increasing their ductility) and relied on mercury as an inert medium. Nitrogen gas was found to have a plasticizing effect on PTFE at pressures of 35 MPa, reducing the modulus of 60% crystalline samples by about 20% [43, 44].

2.3.1.2   Compressive properties

Polymers under compression and tension generally exhibit similar stress-strain characteristics; however, the yield strength is expected to be slightly greater under compression than under tension. The influence of pressure on this stress-differential effect was investigated by Spitzig and Richmond [31] who obtained both tensile and compressive stress-strain measurements for HDPE, determining (at least for this material) that the stress-differential effect is independent of pressure at hydrostatic pressures up to 1100 MPa.

2.3.1.3   Shear properties

Viscoelastic properties of semicrystalline polymers and elastomers at high pressures have been measured by performing dynamic mechanical deformation tests within pressure vessels. Most of them employed a torsion pendulum to achieve oscillatory motion, although other setups have

been used. These measurements were used to determine shear modulus as a function of both pressure and temperature for HDPE [43-45], PA6 [44], PCTFE [44], and PTFE [43, 44]. In all cases, the shear modulus increased with pressure, often linearly [44]. For elastomers, the shear modulus was also found to increase with pressure. Viton B, Neoprene WB, and EPDM were tested in this manner [46]. Generally for isotropic materials the shear modulus is proportional to the elastic modulus, so this behavior is expected.

Dynamic mechanical measurements were also used to investigate time-dependent properties. Stress relaxation and creep measurements have been carried out in polyethylene and in some elastomers [46, 47].

2.3.2 Other mechanical properties at high hydrostatic pressure

Beyond stress-strain testing, information about the effects of high pressure on polymer mechanical properties is fairly limited. We present the available data but cannot say much about trends in these cases.

2.3.2.1 Crack growth and fracture toughness

There is limited data on the influence of high pressure on polymer crack growth and fracture toughness. It has been reported that high pressure increases the resistance to crack propagation in a filled elastomer based on butyl rubber [48]. Lake et al. found that increasing the hydrostatic pressure to 130 MPa reduced crack growth rates in elastomers by nearly three orders of magnitude [49].

Sweeney et al. [50] found no pressure dependence of fracture toughness for polyethylene. Others, however, have found that fracture toughness increases with pressure in epoxies [26, 36] and filled butyl rubber [51].

2.3.2.2 Cyclic loading

Very little published research is available on the effects of high pressure on fatigue for the polymers of interest for hydrogen applications. Cyclic loading experiments are more commonly conducted on composite materials or directly with components, rather than as materials tests on the constituent polymer materials. However, Yamabe et al. have developed a durability tester capable of performing pressure cycling tests in hydrogen at pressures of up to 90 MPa. They visually observed and described crack damage and extrusion fracture in EPDM O-rings under various temperature, pressure, and cycling rate conditions [52, 53]. Crack damage was noticeably worsened by increases in pressure (from 35 to 70 MPa) and temperature (from 60°C to 100°C). Further information about this failure behavior may be found in Section 2.4.2.

The literature contains a number of investigations of failure modes in low-pressure pipes and piping materials. Some of these materials were characterized at relatively high pressures, in fact. Often these samples were subjected to circumferential stresses imposed by an internal pressurizing medium. For example, fatigue of unplasticized PVC water pipes has been investigated as a function of cyclic circumferential stresses up to 50 MPa [54]. The type of failure mode observed, which included different varieties of plastic zone formation and crack growth initiated from different locations, was found to vary with the pressure applied. The researchers found no direct evidence of a stress amplitude below which fatigue failure would not occur. Fatigue and failure of filament-wound GRP pipes have been characterized under cyclic pressures up to several tens of MPa [15, 16, 20].

2.3.2.3 Friction

Towle [55] reported friction coefficients of HDPE as a function of applied load. A rotating anvil shear press was used to apply pressure; the specimens were not subjected to additional hydrostatic pressurization. The friction coefficient was approximately halved by increasing pressure over a 50 MPa range.

2.3.3 Mechanical properties in gaseous hydrogen environments

Mechanical data for polymers in hydrogen are scarce even at relatively low pressures, and the influence of hydrogen on mechanical properties at high pressures has yet to be definitively characterized. Tensile stress-strain relationships have been published for two thermoplastics (PA11 and a bimodal polyethylene) in hydrogen and nitrogen at 3 MPa, as well as atmospheric air, with some additional exploration of the polyethylene material at 5 and 10 MPa [28, 56, 57]. It was concluded that tensile properties were not affected by the presence of hydrogen at pressures up to 10 MPa.

There is no indication that gaseous hydrogen exposure has a measurable effect on the mechanical properties of polymers. Long-term hydrogen exposure at 3 MPa, on the order of one year, did not significantly affect the tensile properties of PA11 or a bimodal polyethylene [28, 57].

2.4 Transport properties

Hydrogen is a relatively small molecule that can dissolve into polymer materials (and other solids) and diffuse through the material. Transport of gases through polymer materials has been extensively studied for a variety of applications. The goal of this review is not to provide an exhaustive review of gas transport in polymer materials, but rather to provide a basic overview of gaseous transport in polymers in the context of high-pressure storage and distribution of gaseous hydrogen. A framework is provided for understanding the basic physics of transport of gases in polymers followed by basic reference data for hydrogen transport properties in materials of interest to the hydrogen energy community.

2.4.1 Permeability, diffusivity and solubility of hydrogen in polymers

2.4.1.1 Description and definitions

In the context of this review, hydrogen transport properties refer to the diffusion of gaseous hydrogen through bulk polymeric material. The polymeric material usually has some functional structure for a specific application as outlined above, such as a liner of a pressure vessel, or an O-ring seal. In general, the polymer structure functions as a barrier to hydrogen transport, although hydrogen can slowly diffuse through the molecular structure of the polymer. This process is characterized by two thermodynamic properties related to the material and the diffusing species: the diffusivity (D) and the solubility (S). The former describes the rate at which a species moves in the material of interest and the latter describes the amount of the species that can be contained within the material. A third property is the product of these two properties and called the permeability (Φ).

Klopffer et al. [58] provide a review of transport properties of gases in polymers. The following is a brief description of the basic parameters and their relationship. Steady-state diffusion in one dimension is idealized by Fick's first law:

$$J = -D\frac{dc}{dx} \tag{2.1}$$

where J is the flux of the diffusing species (in this case hydrogen), c is the concentration of hydrogen and x represents the diffusion direction. For ideal gases in equilibrium with a surface, the concentration of molecular hydrogen is proportional to the partial pressure of hydrogen (p_H):

$$c = Sp_H \tag{2.2}$$

where the proportionality constant is called the solubility (S). This is a special case of Henry's law; in general, the pressure must be replaced by the fugacity, which represents real gas behavior. For a membrane of constant thickness ($t = x_1 - x_2$) across which there is a difference of hydrogen partial pressure ($\Delta p_H = p_{H2} - p_{H1}$), the flux can be expressed as

$$J = -D\frac{(Sp_{H2} - Sp_{H1})}{(x_2 - x_1)} = DS\frac{\Delta p_H}{t} = \Phi\frac{\Delta p_H}{t} \tag{2.3}$$

The permeability (Φ) has units of diffusivity times concentration divided by pressure, which in SI units is mol H_2 (m s Pa)$^{-1}$. Some studies use m^2/s for permeability units; these units appear to represent multiplying the standard unit by RT (where R is the universal gas constant, 8.31447 Pa m^3 (mol K)$^{-1}$, and T is the temperature in Kelvin). In much of the literature related to high-pressure transport the units of mol H_2 (m s MPa)$^{-1}$ are used and this unit is adopted here, since MPa is a more relevant pressure unit for high-pressure systems.

Different isotopes of hydrogen permeate polymers at different rates [59-61]. However, the permeation of hydrogen isotopes in polymers does not follow the dependence associated with classic rate theory (square root of the inverse of mass). Fitch et al. speculate that the difference in diffusion of hydrogen and deuterium is related to the difference in size of the diffusing species. Fitch et al. tested a range of elastomers and the ratio of hydrogen permeability to deuterium permeability was generally between 1.05 and 1.1 [59]. This is important because isotopes of hydrogen are sometimes used in permeation studies to improve resolution of the measurement.

Effect of temperature, pressure and stress
The temperature dependence of the transport properties follows the classic exponential form:

$$A = A_0 \exp\left(\frac{-E_A}{RT}\right) \tag{2.4}$$

where A_0 and E_A are material-dependent constants and A represents the transport property: Φ, D or S. In general, this temperature dependence is followed for polymer materials at low pressure as long as the microstructure of the material is not changing. The effect of high pressure on permeation depends on a number of factors including the imposed stresses and the characteristics of the material. In the limit of ideal sorption (i.e., in the limit of pressure-independent solubility), the effects of hydrostatic pressure on elastomers can be idealized as arising from two opposing effects: (1) the compression of the polymer due to imposed hydrostatic pressure, which reduces diffusion (negative β); and (2) the swelling of the polymer due to hydrogen solubility, which enhances diffusion (positive β). These two effects are combined in a single parameter β and the pressure dependence on permeability [62] is described as

24

$$\Phi = \Phi^* \exp\left(\beta p_H\right) \qquad\qquad\qquad (\,2.5\,)$$

where Φ^* is the permeability in the limit of zero partial pressure. If the pressure does not affect the solubility, then the diffusivity has the same pressure dependence.

While the effect of pressure accounts to some extent for the role of stress, the stress state can be more complicated than achieved in membrane permeation tests and pressures greater than 10 MPa have not been explored for most gases. Just as mechanical properties are affected by imposed stresses, it seems reasonable to presume that stress state plays an important role in transport properties. Indeed, anecdotal information, for example, suggests that the permeation in liners of Type IV pressure vessels (generally HDPE liners) is significantly less than predicted from membrane permeation data. To our knowledge, the effect of stress state on transport properties has not been systematically quantified for polymer materials; however, from a phenomenological perspective, compressive stresses can be idealized as decreasing the β parameter.

The solubility can be a function of pressure, especially at high pressure [63]. Deviations from ideal (pressure-independent) sorption are observed, in particular, for gases with very high solubility, such as CO_2 [64]. Highly soluble gases also display relatively large positive value of the β parameter (~ 0.1 MPa^{-1} for CO_2) [62]. Briscoe et al. relate the magnitude of solubility to the critical temperature of the gas: "high" solubility is observed for gases at temperatures near the critical temperature as in the case of CO_2 at room temperature, while significantly lower solubility is observed for gases with a much lower critical temperature, such as N_2 [64]. Moreover, gases with a lower solubility (e.g., O_2, N_2 and H_2) display small, negative values of β [62], indicating smaller dependency on pressure. Indeed, Terashita et al. measured the effect of pressure on the permeation of N_2 and O_2 in several rubbers and found very small reductions of permeation rates at pressures approaching 10 MPa [65]. While the magnitude of the polymer-hydrogen interactions depend on the chemical character of the polymer (i.e., specific functional groups) as well as the gas [64], high concentrations of gas within the material increase chain mobility, reduce T_g and reduce mechanical strength [64, 66]. This phenomenon is often referred to as plasticization and is well described in the literature for CO_2 at pressures as low as 2 MPa for silicone elastomers [64].

Effect of microstructure and test specimen

Permeation is ideally a bulk property reflecting the microstructure of the test specimen. Thus, permeation will depend on microstructural characteristics, such as orientation, degree of crystallinity, moisture content, filler content, presence of plasticizers, etc. Klopffer et al. review some of the microstructural parameters that affect transport properties in polymers [58]. If test specimens are processed differently from the material used in the application, the test articles may not necessarily reflect permeation in the functional application. Obviously, the integrity of the fabricated specimen itself is also important as well as the uniformity of the dimensions of the specimen (since the thickness of the specimen determines the diffusion distance). The geometry of the permeation specimen can influence the stress state in the material during the test (e.g., an O-ring versus a membrane sample), which may also influence the results. In general, there do not seem to be large (order of magnitude) differences in the transport properties due to testing geometry; differences in the measured transport properties from one study to another can likely

be attributed to differences in the tested materials even though they may be described as the "same" material (e.g., due to differences in additives, fillers, processing conditions, etc.).

2.4.1.2 Test methods for transport properties

There are several test methods that have been employed for reporting permeation in polymer materials. In general, the most common methods use the same principle: pressurize a closed volume where the primary means of pressure drop is permeation through a test specimen (either a thin membrane of polymer, or an O-ring of the material of interest, or the liner of a structure) and measure pressure-volume changes on either or both sides of the specimen. Alternatively, the chemical identity of the diffusing species can be measured directly on the low-pressure side of the polymer by a convenient method, such as a mass spectrometer. Flaconneche et al. review a few methods that are employed in the oil and gas industry [67]. The so-called tritium tracer method is described in Ref. [68], although a similar methodology can be used directly with hydrogen or deuterium. The most common methods employ a thin membrane of material, through which hydrogen diffuses.

ASTM specification D1434 describes standard procedures for determining gas permeability in plastic films (or membranes). A sheet of the test material is mounted so as to form a sealed semi-barrier between two chambers of a gas transmission cell. One chamber is loaded with the test gas at a specific pressure, and the other chamber, at a lower pressure, receives the gas that has permeated through the specimen. The rate of gas transmission through the specimen may be determined by monitoring either pressure or volume changes, or by direct measurement of the chemical identity of the permeating species as a function of time. The test specification distinguishes between (i) geometry-dependent permeance, defined as the ratio of the gas transmission rate per unit area of material to the difference in partial pressure of the gas on the two sides of the film, and (ii) the materials-property called the permeability (Φ), which is the product of the permeance and the film thickness. The ASTM test specification emphasizes that as a bulk material property, permeability must be shown to be constant using several thicknesses of material. In practice, this is rarely done.

2.4.1.3 Hydrogen transport properties in polymers

Hydrogen transport properties at room temperature are listed in Table 2.9 for a range of elastomers. These data include measurements that were made more than 70 years ago as well as more recent measurements. All of these materials show relatively similar hydrogen transport, varying by less than an order of magnitude and generally by less than a factor of two. In short, the effective hydrogen transport properties of elastomers are relatively well known around room temperature and at low pressure (all of these data were obtained at pressure near one atmosphere). That is not to say that some materials cannot show larger differences than shown here; however, we are unaware of relevant elastomeric materials that show hydrogen transport properties that differ from the ones in this table by more than an order of magnitude. Refs. [59, 69-71], in particular, provide transport properties for a wide range of elastomeric materials, including some of the data in Table 2.9.

Hydrogen transport properties of semicrystalline thermoplastics near room temperature are given in Table 2.10. The range of transport properties for these materials is broader than the elastomers, but still relatively narrow. Hydrogen diffusivity tends to be about an order of magnitude lower in the thermoplastics than in the elastomers, while the solubility is relatively

similar. Thus the difference in permeability of the two classes is also about an order of magnitude (since permeability is the product of diffusivity and solubility). These are only very general trends; individual comparisons may yield smaller or greater differences.

There is very little transport data available for epoxies, although we found one study [72] that reports hydrogen permeation in an epoxy as given in Table 2.11. Hydrogen permeation in this epoxy appears to be similar to the thermoplastics. Additionally, sheets (~2 mm thick) of glass fiber-reinforced and carbon fiber-reinforced composite were tested in this same study: permeation of hydrogen through the composite materials was less than measured for the pure epoxy.

Microstructure

As described above, the variation of hydrogen transport properties from one polymer to another is relatively modest (especially considering the many orders of magnitude differences observed for metals [73]). Many of the small differences in transport properties from one study to another for the same material can likely be attributed to microstructural differences (including differences in additives and fillers). While the role of additives and microstructure on gas transport in elastomers has not been extensively studied, several recent studies by Yamabe et al. have investigated the role of fillers in elastomers exposed to high-pressure hydrogen [52, 74-77]. In particular, a study on EPDM shows that changes of hydrogen transport properties due to filler materials are relatively small: the hydrogen diffusivity decreases and the hydrogen solubility increases by factors of up to 2 or 3 with filler (relative to a baseline with no filler) under conditions used in the tests [75]. These changes are attributed to adsorption of hydrogen by the filler material, especially carbon black, which is known to interact strongly with hydrogen [75]. Interaction between filler and dissolved gases clearly depends on the interacting materials; for example, Rutherford et al. report that carbon black filler in EPDM is inert to gas transport for several gases other than hydrogen [78].

Interpretation of the relationship between chemical characteristics of elastomers (and polymers in general) and their transport properties are generally lacking in the literature. In one exception to this, Van Amerongen notes a correlation of lower permeability to higher percentage of acrylonitrile in NBR elastomers, which is attributed to polar groups (as well as methyl groups) generally reducing diffusivity (and permeability) [70].

The properties for PEEK in Table 2.10 provide an example of the effects of microstructure on hydrogen transport in semi-crystalline thermoplastics. While there are likely other microstructure differences in this case (extrusion versus injection or compression molding), the authors suggest that diffusivity and permeability decrease linearly as the crystallinity increases [79]. Greater fraction of crystalline phase (and greater density) results in lower permeation rates in polyethylene also, although hydrogen was not one of the gases used in that study [63]. The crystalline phase is thought to have lower solubility to the permeating species [63] or to be relatively impermeable [79].

Table 2.12 shows the effect of plasticizer on hydrogen transport in PVC, another example of the effects of microstructure. In this case, diffusivity and solubility are relatively constant for low additions of plasticizer, while high additions of plasticizer increase the diffusivity [80]. A study on the effects of plasticizer in PA11 (with gases other than hydrogen) attributes the observed greater diffusivity with the addition of plasticizer to greater mobility of the macromolecular chains without a significant change in solubility [63]. Plasticizers can play a role in hydrogen

transport, but in the few studies that have addressed this phenomenon [63, 80], the effects are relatively modest (much less than an order of magnitude).

In summary, while microstructure, additives and fillers clearly affect hydrogen transport in polymer materials, relatively few studies have systematically investigated the role of microstructure on hydrogen transport. As the examples above illustrate, the few studies that have investigated the role of microstructure on hydrogen transport have shown only modest sensitivity to microstructure: transport properties of the reviewed polymers remain within a relatively narrow range when measured near room temperature and at low pressure.

Aging and microstructural damage

In the context of this work, we use aging to refer to the evolution of the microstructure (e.g., crystallinity, and/or compositional changes) due to exposure to gaseous hydrogen in the range of service temperature and pressure. Microstructural damage refers to changes to the structural integrity due to the evolution of defects such as voids, cracks and delaminations.

While there are relatively few studies of long-term exposure to hydrogen on polymer materials, it is acknowledged that temperature and permeating gas can, in theory, change the microstructure [63]: temperature excursions can affect crystallinity, permeating gases can accelerate loss of volatile additives, etc. In a recent study by Klopffer et al., HDPE and PA11 were aged at temperatures from 20 to 80°C concurrently with hydrogen exposure at pressure up to 2 MPa for times as long as one year [81]. Hydrogen permeability in the aged HDPE and PA11 was unchanged by these aging treatments for these two materials (values are given in Table 2.10 from Ref. [81]).

Rapid gas decompression is one form of damage that can develop during service, which is described in Section 2.4.2. The early-stage evolution of this type of damage and its effects on transport properties have not been illustrated in the literature and are likely less important than developing failure. Structural materials and dynamic seals (such as "soft" seats in valves) are likely to experience mechanical damage in service, although such damage is likely to have more important consequences structurally and functionally. However, there may be cases where permeation could be greatly accelerated without apparent structural or functional failure, such as in composites. Humpenoder investigated the effects of mechanical and thermal cycling on the permeation through composite materials [72]. Thermal cycling of a glass fiber-reinforced composite between room temperature (presumably) and a temperature of 77 K resulted in no change of permeability with helium after 100 cycles. Humpenoder also mechanically cycled the composites in bending at temperature of 77 K and 293 K until the onset of reduced bending modulus, implying the evolution of microstructural damage in the composite. Helium permeation of the "damaged" composites was increased by 30%, suggesting that measurable damage has only a nominal effect on permeation.

Aging and the evolution of service damage in polymers is an important consideration in applications where polymers act as barriers or seals for gaseous hydrogen. Aging and damage (when severe) will impact the function of the system, while from the perspective of hydrogen transport, limited study has not shown significant effects of aging or microstructural damage on hydrogen transport prior to failure.

Temperature

Temperature dependence on transport properties is generally well known, following the classic exponential dependence shown in Equation 2.4. The temperature dependence of permeability and diffusivity for a few select materials is given in Table 2.13, as well as shown in Figure 2.1 and Figure 2.2 respectively. Relative changes in transport properties can be estimated from the exponential term. The enthalpy term associated with permeation is typically between 30 and 40 kJ/mol, although lower values are observed in some cases. Considering a value of 35 kJ/mol for illustration purposes, permeation at a temperature of 358 K (+85˚C) will be an order of magnitude greater than at room temperature (293 K). Relative reductions in permeation at low temperature are somewhat greater: at 233 K (−40˚C) permeation is about 2% of the value at room temperature.

In general, temperature dependent transport properties are reported at elevated temperature and over a very narrow range of temperature, often as small as $\Delta T = 25$˚C (Table 2.13). One report on transport properties at low temperature [72] suggests that the permeability and diffusivity can be extrapolated from elevated temperature data to subambient temperatures at least as low as 200 K.

Pressure and mixed gases

Relatively few of studies have investigated gas permeation in polymers at high pressure (up to about 10 MPa) [62, 65]. In general, at least for these pressures, the effect of pressure on hydrogen permeation is relatively modest and consistent with pressure-independent solubility. Naito et al. measured permeability as a function of pressure (up to about 10 MPa) for several gases in LDPE and PP; for gaseous hydrogen they determined the β parameter (Equation 2.5) to be about (−0.009) MPa^{-1}. Extrapolating these results to a pressure of 70 MPa, the permeability is predicted to be about 50% of the value at one atmosphere. Recent work by Yamabe et al. shows a transition to much larger apparent volume change in EPDM for pressures greater than 10 MPa [53]; however, these measurements were performed after decompression and may represent internal damage, rather than onset of plasticization.

Permeation of gas mixtures in polymers may be important in some applications. Klopffer et al. [82] measured mixtures of hydrogen and methane and determined that the permeation rate of the individual species in HDPE is solely dependent on the partial pressure of the respective gases. Hydrogen mixed with gases that can induce plasticization (i.e., gases with large, positive β values, such as CO_2 [62]) may enhance hydrogen permeation as shown for mixtures of CO_2 and methane [83]. To our knowledge, however, permeation experiments with hydrogen and CO_2 have not been performed.

Table 2.9 Hydrogen transport properties of elastomers near room temperature. Solubility values are generally determined from the definition of permeability and may not be given in the primary reference.

Material	Description	Temp. (K)	$\Phi \times 10^9$ $\left(\dfrac{\text{mol H}_2}{\text{m} \cdot \text{s} \cdot \text{MPa}}\right)$	$D \times 10^{10}$ $\left(\dfrac{\text{m}^2}{\text{s}}\right)$	S^b $\left(\dfrac{\text{mol H}_2}{\text{m}^3 \cdot \text{MPa}}\right)$	Ref.
BR	polybutadiene	298	14	9.6	15	[70, 71]
CR	Neoprene G	298	4.5	3.8	12	[71]
	Neoprene	308	9.2	9.3	10	[59]
EPDM	carbon black filler, antioxidants	308	17	5.0	33	[59]
	several curing agents and antioxidants	293	14	8.0	18	[78]
FKM	Viton E60	308	3.5	1.9	19	[59]
	Viton GF	308	7.3	3.5	21	[59]
NBR	80/20 Perbunan 18	298	8.5	6.4	13	[70]
	73/27 Perbunan	298	5.3	4.5	12	[70]
	Perbunan	298	5.1	4.2	12	[71]
	68/32 Hycar OR 25	298	3.9	3.9	10	[70]
	61/39 Hycar OR 15	298	2.4	2.4	9.8	[70]
IIR	98/2 butyl rubber	298	2.4	1.5	16	[70]
	98/2 butyl rubber[a]	308	4.5	2.9	16	[59]
NIR	74/26	298	2.5	2.5	10	[70]
SBR	Buna S	298	13	10	13	[71]

[a]Average values from four different butyl rubbers.
[b]Solubility values are generally determined from the definition of permeability and may not be given in the primary reference.

Table 2.10 Hydrogen transport properties of semicrystalline thermoplastics near room temperature

Material	Description	Temp. (K)	$\Phi \times 10^9$ $\left(\dfrac{\text{mol H}_2}{\text{m}\cdot\text{s}\cdot\text{MPa}}\right)$	$D \times 10^{10}$ $\left(\dfrac{\text{m}^2}{\text{s}}\right)$	S^b $\left(\dfrac{\text{mol H}_2}{\text{m}^3\cdot\text{MPa}}\right)$	Ref.
HDPE	None given	293	0.82[a]	1.9	4.3	[72]
HDPE	PE XS10B (Total Petrochemical)	293	0.89	—	—	[81]
PE	None given	293	2.4	3.9	6.3	[72]
PE	$\rho = 0.92$, $\alpha \sim 47\text{-}53\%$	Room temp.	3.1	0.47	65	[60]
PE	$\rho = 0.923$ $\rho = 0.9605$	293	2.4 1.0	—	—	[84]
PA	None given	293	0.14[a]	—	—	[72]
PA11	None given	293	0.40	0.65	6.2	[85]
PA11	Rilsan TL	293	0.36	—	—	[81]
PEEK	Extruded, $\alpha = 15\%$	298	1.2	0.53	23	[79]
PEEK	Injection molded, $\alpha = 27\%$	298	0.67	0.52	13	[79]
PEEK	Extruded, $\alpha = 31\%$	298	0.61	0.30	20	[79]
PEEK	Compression molded, $\alpha = 38\%$	298	0.39	0.24	16	[79]
PP	None given	293	3.1	—	—	[84]
PCTFE	None given	293	0.31	—	—	[84]
PTFE	$\rho=2.18$, $\alpha\sim55\text{-}60\%$	298	3.2	—	—	[60]

[a]Value determined by dividing the reported values (given in units of m²/s) by RT

[b]Solubility values are generally determined from the definition of permeability and may not be given in the primary reference.

Table 2.11 Hydrogen transport properties of epoxies and fiber-reinforced composites near room temperature

Material	Description	Temp. (K)	$\Phi \times 10^9$ $\left(\dfrac{\text{mol H}_2}{\text{m}\cdot\text{s}\cdot\text{MPa}}\right)$	$D \times 10^{10}$ $\left(\dfrac{\text{m}^2}{\text{s}}\right)$	S $\left(\dfrac{\text{mol H}_2}{\text{m}^3\cdot\text{MPa}}\right)$	Ref.
Epoxy resin	LY556/HY917 Ciba Geigy	293	0.57[a]	—	—	[72]
GFEP-56	E-glass (56 vol%) + epoxy[b]	293	0.13[a]	—	—	[72]
CFEP-60	C-fiber Toho HTA7 (60 vol%) + epoxy[b]	293	0.18[a]	—	—	[72]

[a]Value determined by dividing the reported values (given in units of m^2/s) by RT
[b]LY556/HY917 Ciba Geigy

Table 2.12 The effects of plasticizer on hydrogen transport properties of PVC near room temperature

Plasticizer	Plasticizer (wt %)	Temp. (K)	$\Phi \times 10^9$ $\left(\dfrac{\text{mol H}_2}{\text{m}\cdot\text{s}\cdot\text{MPa}}\right)$	$D \times 10^{10}$ $\left(\dfrac{\text{m}^2}{\text{s}}\right)$	S^{b} $\left(\dfrac{\text{mol H}_2}{\text{m}^3\cdot\text{MPa}}\right)$	Ref.
—	0	298	0.57	0.50	11	[86]
Not reported	Not reported	293	0.80	—	—	[84]
Not reported	Not reported	293	7.0[a]	3.2	22	[72]
tricresyl triphosphate	0	300	0.80	0.48	17	[80]
	5		0.64	0.46	14	
	10.2		0.59	0.42	14	
	15		0.57	0.44	13	
	20.1		0.72	0.47	15	
	30.8		0.96	1.6	6.1	
	40.0		1.2	2.3	5.4	

[a]Value determined by dividing the reported values (given in units of m^2/s) by RT
[b]Solubility values are generally determined from the definition of permeability and may not be given in the primary reference.

Table 2.13 Relationships for temperature dependence of hydrogen transport properties for some common polymer materials

Material	Description	Temperature Range (K)	Permeability $\Phi = \Phi_o \exp(-H_\Phi / RT)$		Diffusivity $D = D_o \exp(-H_D / RT)$		Solubility[c], $S = \Phi/D$ $S = S_o \exp(-\Delta H_s / RT)$		Ref.
			Φ_o x 10^3 $\left(\dfrac{\text{mol H}_2}{\text{m}\cdot\text{s}\cdot\text{MPa}}\right)$	H_Φ $\left(\dfrac{\text{kJ}}{\text{mol}}\right)$	D_o x 10^6 $\left(\dfrac{\text{m}^2}{\text{s}}\right)$	H_D $\left(\dfrac{\text{kJ}}{\text{mol}}\right)$	S_o $\left(\dfrac{\text{mol H}_2}{\text{m}^3\cdot\text{MPa}}\right)$	ΔH_s $\left(\dfrac{\text{kJ}}{\text{mol}}\right)$	
BR	Poly(butadiene)	298 - 323	0.98[b]	27.6	5.3	21.4	185	6.3	[70]
CR	Neoprene G	288 - 323	4.0	33.9	27	27.6	150	6.3	[71]
IIR	98/2 isobutene/isoprene	298 - 323	5.9[b]	36.4	140	33.9	44	2.5	[70]
NBR	Butadiene/acrylonitrile Perbunan 18 (80/20) Hycar OR 15 (61/39)	298 - 323	1.6[b] 6.9[b]	30.1 36.8	23 92	26.0 31.8	71 75	4.2 5.0	[70]
NIR	74/26 isoprene/acrylonitrile	298 - 323	12[b]	38.1	67	31.0	178	7.1	[70]
SBR	Buna S	298 - 323	1.3	28.5	5.5	21.4	237	7.1	[71]
HDPE	None given	~235 - 300	0.053[a,b]	27	12[b]	27	4.3	0	[72]
PA	None given	~260 - 300	0.0060[a,b]	26	—	—	—	—	[72]
PVC	Unplasticized	298 - 353	0.65	34.5	42	34.5	16	0	[86]
PVC	None given	~210 - 300	0.026[a,b]	20	2.7[b]	22	9.6	-2	[72]
Epoxy	LY556/HY917 Ciba Geigy	Not reported	0.056[a,b]	28	—	—	—	—	[72]

[a]Value determined by dividing the reported values (given in units of m^2/s) by RT (T = 293 K)

[b]Value was calculated from the relationships in this document and additional data in the primary reference.

[c]Solubility values are generally determined from the definition of permeability and may not be given in the primary reference.

Figure 2.1 Temperature dependence of hydrogen permeability of several polymer materials. Temperature relationships and refs. from Table 2.13: BR, IIR, NBR, NIR [70]; CR, SBR [71]; HDPE, PA, epoxy, PVC (low temp. range) [72]; PVC (high temp. range) [86].
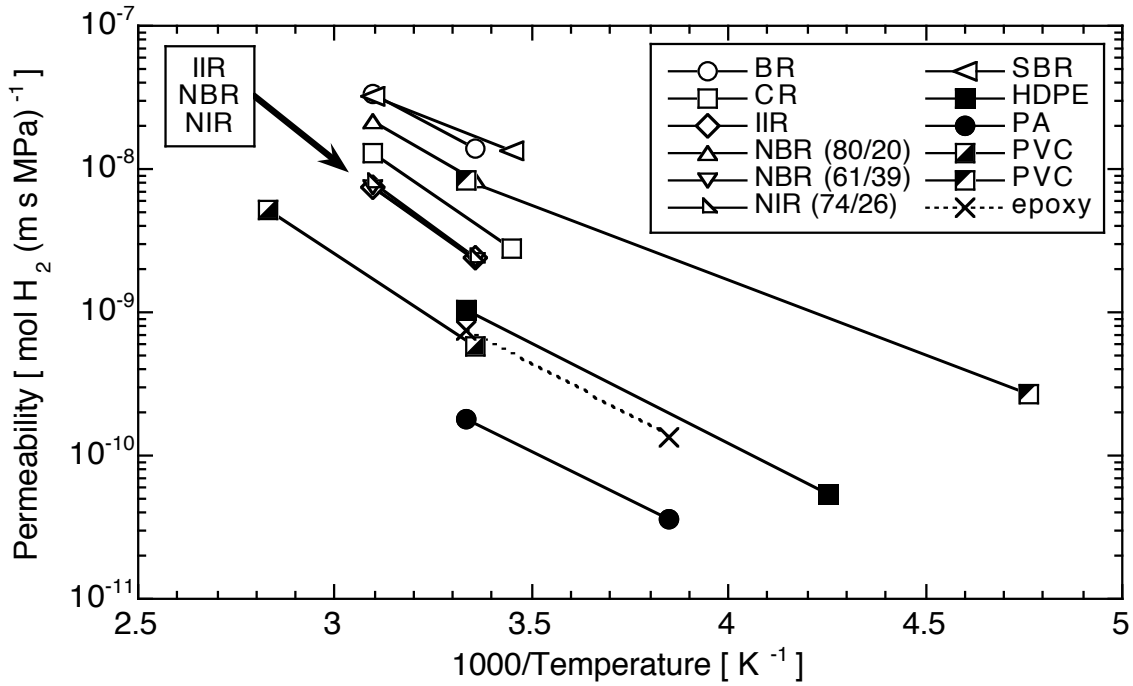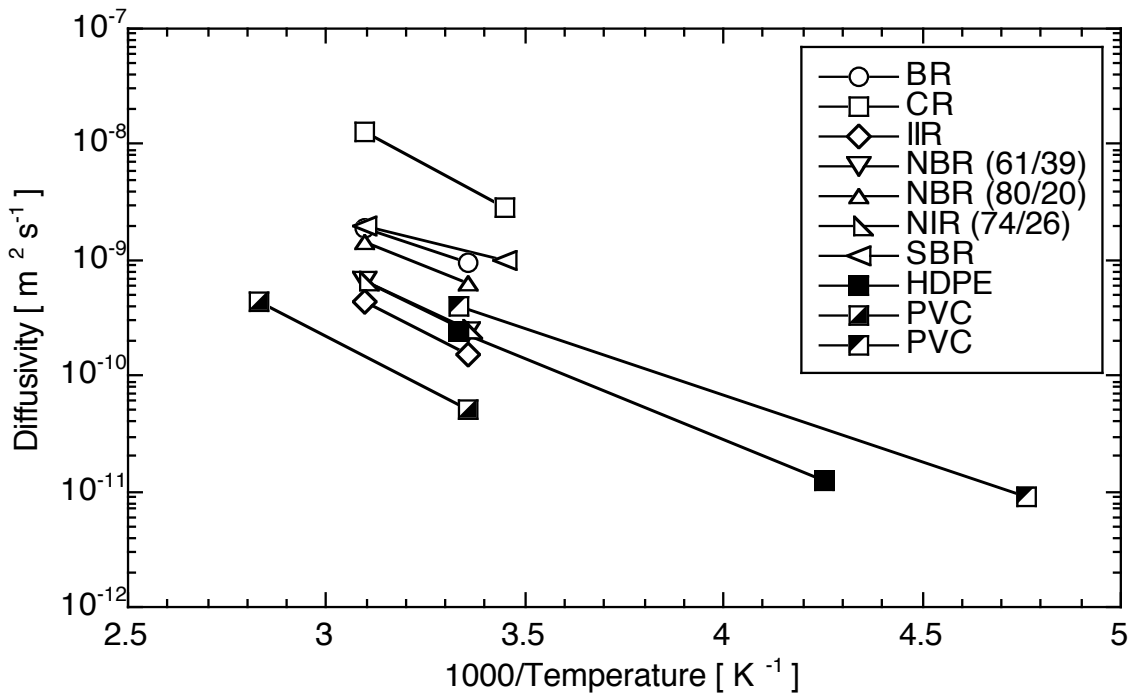

Figure 2.2 Temperature dependence of hydrogen diffusivity of several polymer materials. Temperature relationships and refs. from Table 2.13: BR, IIR, NBR, NIR [70]; CR, SBR [71]; HDPE, PVC (low temp. range) [72]; PVC (high temp. range) [86].

2.4.2 Rapid gas decompression

Rapid gas decompression, also known as explosive decompression, gas-induced rupture, or blister fracture, is a widely recognized phenomenon in polymers. Gas absorbed by a polymer material at high pressure can, upon decompression, cause extensive mechanical damage. A somewhat small set of published decompression data exists, primarily for elastomers in CO_2. However, in recent years, two groups have published work on hydrogen gas decompression effects in elastomers.

2.4.2.1   Description and damage morphology

The overall process of failure induced by rapid gas decompression has been described by several authors [7, 64, 87]. Briefly, at high pressure, a polymer absorbs compressed gas until saturated. Upon release of external pressure, the gas becomes supersaturated, coming out of solution and nucleating at microscopic voids (defects) in the material or at interfaces between polymer and filler particles. As the gas expands, the polymer swells as well, and gas bubbles grow at the nucleation sites. The dissolved gas also escapes from the material at the bulk free surfaces. Both bubble growth and gas escape are diffusion-controlled processes. Irreversible damage occurs when the stresses or strains at bubble walls exceed tearing criteria for the material [88]. Because the gaseous diffusion rate is often much slower than the decompression rate, decompression does not need to be truly rapid in order to cause damage. Decompression with a duration on the order of an hour may cause damage similar to an instantaneous decompression.

Whether and how a material fails upon decompression depends on a number of interacting factors and is generally quite difficult to predict. The concentration of gas in the pressurized material increases with both pressure and the solubility of the gas in the polymer; the higher the gas concentration in the polymer, the greater the stresses induced by decompression. The extent of damage also tends to increase with the magnitude of the pressure drop and the decompression rate. The strength of the material under relevant environmental conditions is important as well. Temperature has a large effect, because the gas solubility and diffusivity have strong temperature dependencies. Koga et al. found that mechanical degradation of decompressed elastomers increased significantly with temperature [52].

The damage morphology can vary considerably, ranging from closed-cell foams [89] to long cracks aligned axially with the sample [52]. Cracking often occurs parallel or perpendicular to the major axes of the specimen. This is because during desorption of the gas, concentration gradients develop causing directionality of cavity propagation relative to the specimen surfaces [90]. Within cylindrical specimens, for example, large concentric cracks parallel to the major cylinder axis may form [91]. These large cracks may coexist with many smaller cracks that tend to be randomly oriented [92]. Cracks often occur in the interior of a specimen only, but they can extend to the exterior surface as well. Jaravel et al. found that the edges of a specimen rarely exhibit damage because, over short distances, it is possible for the decompressed gas to diffuse out of the material over a short time period [90]. Briscoe and Liatsis studied several elastomer/gas combinations and found that surface cracks were produced for only a few systems at high depressurization rates, but that internal cracking occurred in all systems, even at low decompression rates [91].

2.4.2.2   Test methods for rapid decompression

At this time, no standard specifications exist for characterization of rapid gas decompression behavior or the damage caused by it. In the absence of standard test methods, the published research in this area encompasses a variety of characterization methods. These include measurement of mass or volume changes during compression and decompression, tensile or compression testing before and after decompression to demonstrate loss of mechanical integrity, acoustic detection of internal damage, and optical characterization of samples both *in situ* and post-decompression.

2.4.2.3   Effects of decompression on properties

The literature on rapid gas decompression is not extensive, so we summarize it briefly here. Most work has focused on elastomers, which are generally more susceptible to the high mechanical stresses induced by rapid decompression than other polymer materials. The very properties that make them attractive as seals in high-pressure systems, compliance and flexibility, make them both mechanically weaker and subject to higher gas sorption (and therefore greater concentrations of gas to be released upon decompression) than other classes of materials. Of the gases, CO_2 is of prime interest because it is highly soluble in many elastomers, as described in Section 2.4.1.1, and tends to act as a swelling and plasticizing agent, causing volumetric dilation in polymers at high pressures. Comparatively little swelling of the polymer occurs for gases such as N_2 for which hydrostatic compression effects dominate. For example, at 25 MPa, the linear dilation of silicone elastomer has been found to be nearly 20% in CO_2 whereas it is about 1% in N_2 [93].

Briscoe et al. [64] have reviewed aspects of decompression in elastomers in great detail. CO_2 is the most common pressurizing medium studied [87, 88, 91, 92, 94, 95]. Some work has been performed using nitrogen [88], argon [88, 89], and methane [87]. Decompression damage in some thermoplastic materials in CO_2 has been investigated as well, including the semicrystalline materials PP, HDPE, and nylon 6,6 [7, 96], and a variety of amorphous thermoplastics including PVC [97]. In the thermoplastic materials, which were exposed to 20 MPa supercritical CO_2 at 70°C for one hour, the effects of decompression on the mechanical properties of (amorphous) PVC were greater than for semicrystalline polymers [96, 97]. HDPE exhibited negligible change in strength at yield and a few percent reduction in elastic modulus as a result of decompression; PVC exhibited 20% reductions in both strength at yield and elastic modulus.

For hydrogen gas, the published work on rapid gas decompression has been limited to elastomers. Yamabe et al. [74, 98, 99] have characterized EPDM, VMQ, and HNBR decompressed from hydrogen pressures of up to 10 MPa at 30°C, measuring hydrogen release profiles, optically assessing crack size as a function of time after decompression and assessing the effect of various fillers on blister damage. Damage was found to be less severe in silica-filled composites than in elastomers without fillers. Cracks formed in EPDM samples that were decompressed from hydrogen pressures of 2 MPa or greater. The effect of filler depends to a great extent on the quality of the interface between the filler particles and the polymer matrix; particles having weak interactions with the matrix material can debond and act as sites for gas accumulation, while strong interfaces can reduce overall gas sorption by hindering gas sorption by the material [93]. Sorption of hydrogen by the filler (as described in Section 2.4.1.3) could further enhance debonding because this is likely to increase hydrogen gas concentrations at the filler surfaces.

Yamabe and colleagues used design of experiments to assess the relative importance of parameters affecting decompression failure of O-rings in hydrogen [52]. This study is of particular interest because it utilized a high-pressure hydrogen durability testing apparatus capable of operating at hydrogen pressures as high as 90 MPa. The O-ring materials selected were once again EPDM, VMQ, and HNBR and contained unspecified fillers. Damage to the material was assessed by measuring the tensile force required to fracture the specimen before and after 10 pressure cycles. In most cases, the final fracture force was at least 80% of the initial fracture force. However, samples cycled to 90 MPa at 100°C exhibited fracture forces of 30-50% of the initial fracture force. The researchers found that increasing temperature and decreasing decompression time (which is not the same as decompression rate due to the variable pressure ranges used) caused more severe damage. They found that VMQ exhibited the slightest damage and identified an optimal filler concentration for resistance to cracking. In subsequent work they continued their investigations of EPDM materials cycled under high-pressure hydrogen by optically characterizing crack damage [53].

Jaravel et al. [90, 100] characterized a modified silicone elastomer decompressed from hydrogen pressures up to 27 MPa. Specimens, which were transparent, were visually tracked during decompression to determine the time at which the first visible damage occurred. They found that higher saturation pressures and faster decompression rates led to earlier onset of blistering. Tensile loading of the sample also increased the rate at which damage occurred. The elastomer remained undamaged at decompression rates below 0.2 MPa/min if the saturation pressure of the gas was kept sufficiently low (9 MPa). The decompression rate could be increased if the saturation pressure of the hydrogen gas was decreased [90].

The studies of rapid gas decompression in hydrogen discussed above represent a good initial assessment of the phenomenon, but a systematic understanding is lacking, especially for high pressures and relatively slow decompression rates. Our understanding of rapid gas decompression in general is limited by the complexity and variety of the physics involved and remains an area of scientific interest.

2.5 Test methods

While standards exist for the measurement of many properties of polymer materials, we are unaware of standardized test methods for evaluating polymer materials in the presence of hydrogen at high pressure. Standards for qualifying polymer-based equipment for high-pressure hydrogen service do exist, for example, for hydrogen fuel systems containing fiber-reinforced plastic pressure vessels (e.g., SAE J2579, Standard for Fuel Systems in Fuel Cell and Other Hydrogen Vehicles). There are also numerous standards for plastic pressure pipe (e.g., ASTM D2992, Standard Test Method for Obtaining Hydrostatic or Pressure Design Basis for "Fiberglass" [Glass-Fiber-Reinforced Thermosetting-Resin] Pipe and Fittings). However, tests for polymer *material* properties (as opposed to the properties of polymer *devices*) in high-pressure hydrogen environments remain non-standardized.

While there have been some efforts to measure the properties of polymer materials in high-pressure environments or in gaseous hydrogen environments, these efforts have been, in general, topics of research. Consequently, equipment, methods and procedures have been developed independently by individual research groups without standardization. Several groups around the world, for example, have been actively studying the physical interactions of gaseous hydrogen

with polymer materials as well as the degradation processes associated with pressure cycling: particularly, elastomers in Japan [52, 53, 74-77, 98, 99] and semicrystalline thermoplastics and elastomers in France [28, 56, 57, 81, 90, 100]. These groups have independently developed their own equipment and methods for evaluating materials in hydrogen environments, although measurement of standard properties (such as tensile properties of polymers) is based on standard practice for measuring such properties in air. Similarly, measurement of the effects of hydrostatic stress on polymer materials has also been confined to the laboratory and not been applied to industrial practice, thus the details of testing by different research laboratories can vary significantly. Standard procedures for evaluating other polymer characteristics (such as damage tolerance due to pressure cycling, i.e., rapid gas decompression) do not exist.

Hydrogen transport properties in polymer materials are an exception to the lack of standard practices for evaluating materials for hydrogen service. Measurement of gas permeation in polymers is a broad topic affecting many industries, thus a method for gas permeation measurements has been standardized in ASTM D1434 (and likely other documents as well). This method, however, is limited in scope and does not account for the specific configurations and applications of polymer materials for high-pressure hydrogen service.

In summary, methods of measuring properties of polymer materials in high-pressure hydrogen environments are lacking. Moreover, metrics for quantifying the effects of hydrogen are also missing; these may include specific criteria (e.g., properties) for hydrogen service and/or design methods that incorporate measured properties in the design of components for hydrogen service.

3   GAP ANALYSIS

In this section we attempt to identify the major gaps in knowledge and data for polymers potentially useful for hydrogen service. These gaps are based on information that seemed to be missing during our compilation of Section 2 of this report yet relevant to the use cases described in Section 1. We emphasize that the gaps identified here pertain to scientific knowledge about classes of polymeric materials. This analysis does not extend to assessing the performance of engineered devices beyond material considerations.

First, we describe the gaps by category. We then organize the gaps we have identified based on their relative value to hydrogen applications and the resources required to fill the gap. Finally, we make some additional comments related to temperature that we do not believe constitute gaps but may be worthy of consideration in the future.

3.1   Gaps by category

3.1.1   Fundamental physics and broad trends

The effects of high pressure (i.e., >10 MPa) on hydrogen transport properties in polymers have not been investigated. Pressure-independent solubility can be inferred from study of elastomers [74] and semicrystalline thermoplastics [62, 65] at pressures up to about 10 MPa with moderate reduction of permeation rates. Deviations from these ideal behaviors may be associated with plasticization of the polymer by the gas. Plasticization has important implications on the physical and mechanical properties of the materials, including reduced T_g and reduced strength as well as enhancing gas transport in the polymer. Some evaluation of a range of representative materials in high-pressure gaseous hydrogen is necessary to assess the potential for plasticization; assessment of plasticization could also be performed by measuring mechanical properties or physical properties in high-pressure gaseous hydrogen.

Polymers have been fairly well characterized at extremely high pressure (>100 MPa) in non-permeating environments. The basic dependence of T_g on pressure and the variation of mechanical properties with pressure are relatively well understood. The available data demonstrate that high hydrostatic pressure increases T_g and improves the mechanical strength of polymers. Because this trend has been established, and the strength at atmospheric pressure constitutes a lower bound, it seems that additional high-pressure characterization of conventional materials would have relatively little value in the absence of hydrogen exposure.

Rapid gas decompression has been investigated in several elastomers in hydrogen environments, although pressures in the neighborhood of 100 MPa have rarely been used [52]. Damage clearly evolves in elastomers subjected to pressure cycling, although knowledge of the mechanisms of damage is still evolving. The combined effects of temperature and pressure cycling have not been evaluated, although it seems reasonable to presume that temperature cycling can result in similar damage evolution due to the thermal dependency of hydrogen solubility. Standardized methods for evaluating rapid gas decompression are also needed, along with metrics for assessing the resistance of materials to this type of damage. Rapid decompression of thermoplastics, in particular, has not been thoroughly investigated.

3.1.2 Incomplete characterization of materials

The effect of high-pressure gaseous hydrogen on fracture and fatigue in polymer materials is unknown. New data obtained in this area would represent a significant advance.

The friction and wear properties of polymers in gaseous hydrogen have not been characterized in the open literature. Friction and wear is important in compressors, valves and other actuated devices. Methods for characterizing wear properties, in general, are poorly standardized and facilities for performing measurements in high-pressure environments are likely non-existent. Characterization techniques and facilities will become a critical gap if failure modes associated with friction and wear are demonstrated.

Hydrogen transport data at low pressure are missing for several polymers, in particular epoxies and composite materials. Because hydrogen transport properties for polymers fall into a relatively narrow window, significant additions to the available conventional data are not critical. Many questions, however, remain, such as effects of (i) aging, (ii) imposed stress state, (iii) extrapolation to low temperature, (iv) extrapolation to high pressure, and (v) the combination of these effects. Studies on permeation in components have been investigated and show significant differences between permeation measurements using membrane specimens and permeation in components, but these studies have not been published in the open literature. A scientific basis for translating materials properties to engineering design is also needed.

In fuel cell applications, the hydrogen fuel has very low levels of contaminants (typically a few part per million). Thus, trace contaminants likely will be unimportant for fuel applications. In some distribution scenarios, contaminants can be important; these scenarios appear to be low-pressure applications and the contaminants are likely similar to those encountered in natural gas distribution. Experience from natural gas should provide sufficient basis for understanding the role of contaminants on the behavior of polymers. For high-pressure applications, potential for volatiles from polymer materials entering the hydrogen stream remains an unknown.

3.1.3 Test method gaps

Testing in high-pressure gaseous hydrogen is expensive and time-consuming. Few facilities for this purpose exist. Standard test methods even for straightforward experiments may require modification due to changes to safety protocols, limitations on specimen sizes imposed by the volume of pressure chambers, and so forth. For characterization of basic properties, the fundamental methods remain the same (e.g., CSA CHMC1-12—Test methods for evaluating material compatibility in compressed hydrogen applications: Phase 1, metals—adopts standard methods for measurement of mechanical properties of metals and applies additional requirements specific to testing in hydrogen environments; there is a desire to expand this CSA document to include polymers). However, it is not clear that the mechanical information compiled in this document pertains directly to the modes of failure observed in hydrogen systems. In fact, the failure modes of polymer materials have not been systematically categorized or characterized. The physical basis of many failure modes may be complex and our understanding of them may not be well developed. Development of experiments and metrics to characterize the failure modes and the susceptibility of the materials to these failures would be of great value.

Standard test methods should be developed for rapid gas decompression. Standardization is needed in many areas, including preparation and equilibration of test specimens, identification of the experimental parameters to be controlled, timescales of the experiments, assessment of

damage, and types of information to collect and report. Furthermore, the effect of pressure cycling on rapid gas decompression is of interest, and methods should be established for this as well.

3.2 Schematic organization of gaps

We have placed the major gaps from the previous section onto a two-dimensional set of axes (Figure 3.1), mapping the approximate importance to hydrogen systems of each gap against the resources required to overcome it. We have divided the plot into quadrants because the precision in this analysis is low. In arranging the gaps on this plot, we assumed that measurements made in high-pressure gaseous hydrogen environments require extensive resources, and that measurements in low-pressure hydrogen environments require relatively few resources.
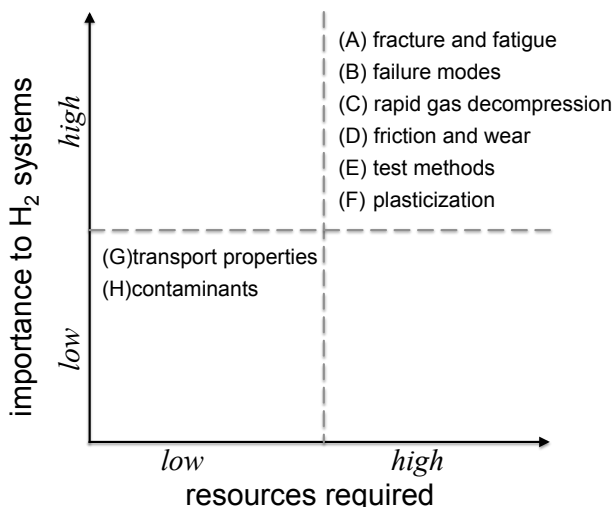

Figure 3.1 Schematic organization of gaps

The gaps, lettered (A) through (H), are as follows. All have been discussed in greater detail in the previous section.

(A) Fracture and fatigue: The influence of high-pressure gaseous hydrogen (up to 100 MPa) on fracture and fatigue of polymers is unknown.

(B) Failure modes: The modes of failure of polymer materials in high-pressure gaseous hydrogen have been neither categorized nor characterized. A workshop to survey the experience of industry would be exceptionally helpful to initiate assessment of failure modes. Subsequent experimental work to recreate and characterize failures is likely to require significant resources.

(C) Rapid gas decompression: This failure mode is widely acknowledged; however, a fundamental understanding of the failure process (and damage evolution) is lacking. Methodologies to evaluate damage evolution in polymers due to pressure cycling and establish design life are also missing.

(D) <u>Friction and wear</u>: High-pressure gaseous hydrogen affects friction and wear of polymer materials. Methodologies to evaluate and characterize friction and wear need development.

(E) <u>Test methods</u>: Standardized methodologies to evaluate and qualify materials for resistance to known failure modes are lacking.

(F) <u>Plasticization</u>: The phenomenon of plasticization of polymers due to sorption of certain gases is well known. Plasticization strongly impacts physical and mechanical properties; therefore, a few representative materials should be evaluated in gaseous hydrogen at pressures up to 100 MPa to determine if plasticization can be induced by high concentrations of hydrogen.

(G) <u>Transport properties</u>: In general, hydrogen transport properties (permeability, diffusivity, solubility) are well known. A few material classes (e.g., epoxies) need additional characterization.

(H) <u>Contaminants</u>: The effects of trace contaminants on polymer properties and potential off-gassing of mobile or volatile species from polymer materials should be characterized.

3.3 Additional considerations

3.3.1 Temperature effects

It is important to recall that despite this document's focus on the effects of high pressure and hydrogen and the corresponding lack of emphasis on temperature-related information, polymer properties are highly sensitive to temperature. Temperature is likely to have a large impact on the properties of polymer materials in hydrogen infrastructure and vehicle fuel systems. We do not consider this a gap because the effects of temperature on polymer properties tend to be well understood. However, when characterizing materials under specific conditions and failure modes relatively unique to hydrogen systems, a reassessment of the combined effects of temperature and pressure in hydrogen environments may be valuable.

3.3.2 Liquid hydrogen environments

The use of polymers in cryogenic (liquid) hydrogen systems at 20 K (−250°C) has not been a focus of this document. This is because most polymers become brittle at temperatures well above 20 K and are not suitable for cryogenic service. Therefore, metals are extensively used in applications involving exposure to cryogenic temperatures. However, polymers and polymer composites (usually based on Teflon or nylon) have historically been used in liquid hydrogen environments as seals and bearings in rockets and space applications. These applications were generally short-lived (on the order of minutes). Characterizing and selecting polymer materials intended for long-term exposure to liquid hydrogen, as would be needed for cryogenic storage systems, could be a much greater challenge.

There have been efforts, particularly in the aerospace arena, to develop lightweight composite tanks for liquid hydrogen storage. Polymers have also been experimentally investigated as cryogenic liner materials [101]. Other researchers have investigated the performance of polymers and polymer composites for their potential use as fittings, seals and solid lubricants in liquid hydrogen environments [102, 103]. We are under the impression that these efforts have not

sufficiently progressed beyond the research stage, thus they cannot yet be considered as viable alternatives to established materials for liquid hydrogen storage.

4 REFERENCES

1. Weber, M. and J. Perrin, *Hydrogen transport and distribution*, in *Hydrogen Technology: Mobile and Portable Applications*, A. Leon, Editor. 2008, Springer. p. 129-149.
2. *Hydrogen standardization interim report for tanks, piping, and pipelines (STP/PT-003)*, ASME Standards Technology, LLC: New York.
3. Maus, S., et al., *Filling procedure for vehicles with compressed hydrogen tanks.* Int. J. Hydrogen Energy, 2008. **33**: p. 4612-4621.
4. Wolf, J., *Liquid-hydrogen technology for vehicles.* MRS Bull., 2002. **27**: p. 684-687.
5. Dicken, C.J.B. and W. Merida, *Measured effects of filling time and initial mass on the temperature distribution within a hydrogen cylinder during refuelling.* J. Power Sources, 2007. **165**: p. 324-336.
6. Cumalioglu, I., et al., *State of the art: hydrogen storage.* J. Fuel Cell Sci. Technol., 2008. **5**: p. 034001-1-034001-10.
7. Lorge, O., B.J. Briscoe, and P. Dang, *Gas induced damage in poly(vinylidene fluoride) exposed to decompression.* Polymer, 1999. **40**: p. 2981-2991.
8. Sperling, L.H., *Introduction to Physical Polymer Science*. 2005: John Wiley & Sons.
9. Jones Parry, E. and D. Tabor, *Effect of hydrostatic pressure on the mechanical properties of polymers: a brief review of published data.* J. Mater. Sci., 1973(8): p. 1510-1516.
10. Martienssen, W. and H. Warlimont, eds. *Springer Handbook of Condensed Matter and Materials Data*. 2005, Springer.
11. Andrews, R.J. and E.A. Grulke, *Glass transition temperatures of polymers*, in *Polymer Handbook*, J. Brandrup, E.H. Immergut, and E.A. Grulke, Editors. 1999, John Wiley & Sons.
12. Pai, P.C.-H. and D.J. Meier, *The effect of pressure on the ultimate properties of elastomers.* Rubber Chem. Technol., 1992. **65**: p. 396-410.
13. Seeger, A., et al., *Melting point of polymers under high pressure part i. influence of the polymer properties.* Thermochim. Acta, 2004. **424**: p. 175-181.
14. Miyamoto, Y., C. Nakafuku, and T. Takemura, *Crystallization of poly(chlorotrifluoroethylene).* Polym. J., 1972. **3**: p. 122-128.
15. Hull, D., M.J. Legg, and B. Spencer, *Failure of glass/polyester filament wound pipe.* Composites, 1978. **9**: p. 17-24.
16. Owen, M.J. and J.R. Griffiths, *Evaluation of biaxial stress failure surfaces for a glass fabric reinforced polyester resin under static and fatigue loading.* J. Mater. Sci., 1978. **13**: p. 1521-1537.
17. Wronski, A.S. and T.V. Parry, *Compressive failure and kinking in uniaxially aligned glass-resin composite under superposed hydrostatic pressure.* J. Mater. Sci., 1982. **17**: p. 3656-3662.
18. Sigley, R.H., A.S. Wronski, and T.V. Parry, *Tensile failure of pultruded glass-polyester composites under superimposed hydrostatic pressure.* Composites Sci. Technol., 1991. **41**: p. 395-409.
19. Sigley, R.H., A.S. Wronski, and T.V. Parry, *Axial compressive failure of glass-fibre polyester composites under superposed hydrostatic pressure: influence of fibre bundle size.* Composites Sci. Technol., 1992. **43**: p. 171-183.
20. Samanci, A., et al., *Fatigue crack growth of filament wound GRP pipes with a surface crack under cyclic internal pressure.* J. Mater. Sci., 2008. **43**: p. 5569-5573.

21.   Arikan, H., *Failure analysis of (±55°)3 filament wound composite pipes with an inclined surface crack under static internal pressure.* Composite Structures, 2010. **92**: p. 182-187.

22.   Gemi, L., et al., *Progressive fatigue failure behavior of glass/epoxy (±75)2 filament-wound pipes under pure internal pressure.* Materials and Design, 2009. **30**: p. 4293-4298.

23.   Weaver, C.W. and J.G. Williams, *Deformation of a carbon-epoxy composite under hydrostatic pressure.* J. Mater. Sci., 1975. **10**: p. 1323-1333.

24.   Rhee, K.Y., et al., *Fracture behavior of seawater-absorbed carbon/epoxy laminated composites in the hydrostatic pressure condition.* Mater. Sci. Eng. A, 2006. **419**: p. 209-213.

25.   Yuan, J., et al., *The effect of high pressure on the mechanical behavior of short fiber composites.* Polym. Eng. Sci., 1984. **24**: p. 844-850.

26.   Li, D., et al., *Fracture behavior of unmodified and rubber-modified epoxies under hydrostatic pressure.* J. Mater. Sci., 1994. **29**: p. 2205-2215.

27.   Hoppel, C.P.R., T.A. Bogetti, and J.W. Gillespie, Jr., *Effects of hydrostatic pressure on the mechanical behavior of composite materials, ARL-TR-727*, 1995, Army Research Laboratory.

28.   Castagnet, S., et al., *Hydrogen influence on the tensile properties of mono and multi-layer polymers for gas distribution.* Int. J. Hydrogen Energy, 2010. **35**(14): p. 7633-7640.

29.   Tsirule, K.I. and E.L. Tyunina, *Viscoelastic and deformational properties of polymers under high pressure*, in *High-pressure Chemistry and Physics of Polymers*, A.L. Kovarskii, Editor. 1994, CRC Press.

30.   Sauer, J.A., *Deformation, yield and fracture of polymers at high pressure.* Polym. Eng. Sci., 1977. **17**: p. 150-164.

31.   Spitzig, W.A. and O. Richmond, *Effect of hydrostatic pressure on the deformation behavior of polyethylene and polycarbonate in tension and in compression.* Polym. Eng. Sci., 1979. **19**: p. 1129-1139.

32.   Mears, D.R., K.D. Pae, and J.A. Sauer, *Effects of hydrostatic pressure on the mechanical behavior of polyethylene and polypropylene.* J. Appl. Phys., 1969. **40**: p. 4229-4237.

33.   Yoon, H.N., K.D. Pae, and J.A. Sauer, *The effects of combined pressure-temperature on mechanical behavior of polypropylene.* J. Polym. Sci. Polym. Phys. Ed., 1976. **14**: p. 1611-1627.

34.   Yuan, J., A. Hiltner, and E. Baer, *The mechanical properties of PVC under high pressure.* J. Mater. Sci., 1983. **18**: p. 3063-3071.

35.   Davis, L.A. and C.A. Pampillo, *Kinetics and deformation of PTFE at high pressure.* J. Appl. Phys., 1972. **43**: p. 4285-4293.

36.   Wronski, A.S. and T.V. Parry, *Fracture of a plasticized epoxide under superposed hydrostatic pressure.* J. Mater. Sci., 1982. **17**: p. 2047-2055.

37.   Vroom, W.I. and R.F. Westover, *Properties of polymers at high pressure.* SPE J., 1969. **25**: p. 58-61.

38.   Pugh, H.L.D., et al., *The effect of hydrostatic pressure on the tensile properties of plastics.* Polym. Eng. Sci., 1971. **11**: p. 463-473.

39.   Pae, K.D. and D.R. Mears, *The effects of high pressure on mechanical behavior and properties of polytetrafluoroethylene and polyethylene.* Polym. Lett., 1968. **6**: p. 269-273.

40.   Paterson, M.S., *Effect of pressure on Young's modulus and the glass transition in rubbers.* J. Appl. Phys., 1964. **35**: p. 176-179.

41.   Matsushige, K., S.V. Radcliffe, and E. Baer, *The mechanical behavior of poly(methyl methacrylate) under pressure.* J. Polym. Sci. Polym. Phys. Ed., 1976. **14**: p. 703-721.

42.   Trent, J.S., et al., *Effects of environment on the mechanical properties of plastics under high pressure.* Polym. Eng. Sci., 1978. **18**: p. 1235-1239.

43.   Billinghurst, P.R. and D. Tabor, *The effect of hydrostatic pressure on the visco-elastic properties of polymers.* Polymer, 1971. **12**: p. 101-118.

44.   Jones Parry, E. and D. Tabor, *Pressure dependence of the shear modulus of various polymers.* J. Mater. Sci., 1974. **9**: p. 289-292.

45.   Truss, R.W., R.A. Duckett, and I.M. Ward, *Effect of hydrostatic pressure on the yield and fracture of polyethylene in torsion.* J. Mater. Sci., 1981. **16**: p. 1689-1699.

46.   Fillers, R.W. and N.W. Tschoegl, *The effect of pressure on the mechanical properties of polymers.* Trans. Soc. Rheol., 1977. **21**: p. 51-100.

47.   Kralj, A., T. Prodan, and I. Emri, *An apparatus for measuring the effect of pressure on the time-dependent properties of polymers.* J. Rheol., 2001. **45**: p. 929-943.

48.   Zezin, Y.P., *Effect of hydrostatic pressure on the viscosity of failure of polymeric materials.* Mech. Composite Mater., 1987. **22**: p. 664-668.

49.   Lake, G.J., A.G. Thomas, and C.C. Lawrence, *Effects of hydrostatic pressure on crack growth in elastomers.* Polymer, 1992. **33**: p. 4069-4074.

50.   Sweeney, J., R.A. Duckett, and I.M. Ward, *Fracture toughness of a tough polyethylene using tension testing in a high-pressure environment.* J. Mater. Sci. Lett., 1986. **5**: p. 1109-1110.

51.   Zezin, M.Y. and Y.P. Zezin, *Effect of hydrostatic pressure on the rate dependence of the fracture toughness of high-filled polymeric materials.* Strength Mater., 2001. **33**: p. 224-229.

52.   Koga, A., et al., *Evaluation on high-pressure hydrogen decompression failure of rubber O-ring using design of experiments.* Int. J. Automotive Eng., 2011. **2**: p. 123-129.

53.   Yamabe, J., A. Koga, and S. Nishimura, *Failure behavior of rubber O-ring under cyclic exposure to high-pressure hydrogen gas.* Eng. Failure Anal., 2013. **in press.**

54.   Joseph, S.H. and P.S. Leevers, *Failure mechanics of uPVC cyclically pressurized water pipelines.* J. Mater. Sci., 1985. **20**: p. 237-245.

55.   Towle, L.C., *Shear strength and friction measurements on polyethylene under high pressure.* J. Appl. Phys., 1973. **44**: p. 1611-1615.

56.   Castagnet, S., et al., *Mechanical testing of polymers in pressurized hydrogen: tension, creep and ductile fracture.* Exp. Mech., 2011. **52**: p. 229-239.

57.   Castagnet, S., et al., *Effect of long-term hydrogen exposure on the mechanical properties of polymers used for pipes and tested in pressurized hydrogen.* Int. J. Pressure Vessels Piping, 2012. **89**: p. 203-209.

58.   Klopffer, M.H. and B. Flaconneche, *Transport properties of gases in polymers: bibliographic review.* Oil Gas Sci. Technol. - Rev. IFP, 2001. **56**: p. 223-244.

59.   Fitch, M.W., et al., *Permeation of several gases through elastomers, with emphasis on the deuterium/hydrogen pair.* J. Appl. Polym. Sci., 1993. **47**: p. 1033-1046.

60.   Miyake, H., et al., *Permeation, diffusion, and solution of hydrogen isotopes, methane, and inert gases in/through tetrafluoroethylene and polyethylene.* J. Vac. Sci. Technol. A, 1983. **1**: p. 1447-1451.

61.   Agrinier, P., et al., *Permeation selectivity of gaseous isotopes through dense polymers: peculiar behavior of the hydrogen isotopes.* J. Membrane Sci., 2008. **318**: p. 373-378.

62.   Naito, Y., et al., *The effect of pressure on gas permeation through semicrystalline polymers above the glass transition temperature.* J. Polym. Sci. Part B Polym. Phys., 1991. **29**: p. 457-462.

63.   Flaconneche, B., J. Martin, and M.H. Klopffer, *Permeability, diffusion and solubility of gases in polyethylene, polyamide 11 and poly(vinylidene fluoride).* Oil Gas Sci. Technol. - Rev. IFP, 2001. **56**: p. 261-278.

64.   Briscoe, B.J., T. Savvas, and C.T. Kelly, *Explosive decompression failure of rubbers: a review of the origins of pneumatic stress induced rupture in elastomers.* Rubber Chem. Technol., 1994. **67**: p. 384-416.

65.   Terashita, F., et al., *Airtight butyl rubber under high pressures in the storage tank of CAES-G/T system power plant.* J. Appl. Polym. Sci., 2005. **95**: p. 173-177.

66.   Zhang, Z. and Y.P. Handa, *An in situ study of plasticization of polymers by high-pressure gases.* J. Polym. Sci. Part B Polym. Phys., 1998. **36**: p. 977-982.

67.   Flaconneche, B., J. Martin, and M.H. Klopffer, *Transport properties of gases in polymers: experimental methods.* Oil Gas Sci. Technol. - Rev. IFP, 2001. **56**: p. 245-259.

68.   Stodilka, D.O., et al., *A tritium tracer technique for the measurement of hydrogen permeation in polymeric materials.* Int. J. Hydrogen Energy, 2000. **25**: p. 1129-1136.

69.   Barrer, R.M., *Permeation, diffusion and solution of gases in organic polymers.* Trans. Faraday Soc., 1939. **35**: p. 628-643.

70.   Van Amerongen, G.J., *Influence of structure of elastomers on their permeability to gases.* J. Polym. Sci., 1950. **5**: p. 307-332.

71.   Van Amerongen, G.J., *The permeability of different rubbers to gases and its relation to diffusivity and solubility.* J. Appl. Phys., 1946. **17**: p. 972-985.

72.   Humpenoder, J., *Gas permeation of fibre reinforced plastics.* Cryogenics, 1998. **38**: p. 143-147.

73.   Causey, R.A., R.A. Karnesky, and C. San Marchi, *Tritium barriers and tritium diffusion in fusion reactors*, in *Comprehensive Nuclear Materials*, J.M. Konings, Editor. 2011, Elsevier: Oxford. p. 511-549.

74.   Yamabe, J. and S. Nishimura, *Influence of fillers on hydrogen penetration properties and blister fracture of rubber composites for O-ring exposed to high-pressure hydrogen gas.* Int. J. Hydrogen Energy, 2009. **34**: p. 1977-1989.

75.   Yamabe, J. and S. Nishimura, *Influence of carbon black on decompression failure and hydrogen permeation properties of filled ethylene-propylene-diene-methylene rubbers exposed to high-pressure hydrogen gas.* J. Appl. Polym. Sci., 2011. **122**: p. 3172-3187.

76.   Yamabe, J., et al., *Blister fracture of rubbers for O-ring exposed to high pressure hydrogen gas*, in *Effects of Hydrogen on Materials: Proceedings of the 2008 International Hydrogen Conference*, B.P. Somerday, P. Sofronis, and R. Jones, Editors. 2009, ASM International. p. 389-396.

77.   Koga, A., et al., *A study of blister damages of rubber O-ring by high pressure hydrogen durability tester*, in *Effects of Hydrogen on Materials: Proceedings of the 2008 International Hydrogen Conference*, B.P. Somerday, P. Sofronis, and R. Jones, Editors. 2009, ASM International. p. 397-404.

78.   Rutherford, S.W., et al., *Measurement and correlation of sorption and transport properties of ethylene-propylene-diene monomer (EPDM) elastomers.* J. Membrane Sci., 2005. **263**: p. 57-65.

79. Monson, L., S.I. Moon, and C.W. Extrand, *Permeation resistance of poly(ether ether ketone) to hydrogen, nitrogen, and oxygen gases.* J. Appl. Polym. Sci., 2013. **127**: p. 1637-1642.

80. Sefcik, M.D., et al., *Diffusivity of gases and main-chain cooperative motions in plasticized poly(vinyl chloride).* J. Polym. Sci. Polym. Phys. Ed., 1983. **21**: p. 1041-1054.

81. Klopffer, M.H., et al., *New materials for hydrogen distribution networks: materials development and technico-economic benchmark.* Defect and Diffusion Forum, 2012. **323-325**: p. 407-412.

82. Klopffer, M.H., B. Flaconneche, and P. Odru, *Transport properties of gas mixtures through polyethylene.* Plastics, Rubber and Composites, 2007. **36**: p. 184-189.

83. Jordan, S.M. and W.J. Koros, *Permeability of pure and mixed gases in silicone rubber at elevated pressures.* J. Polym. Sci. Part B Polym. Phys., 1990. **28**: p. 795-809.

84. Ito, Y., *The permeability of gases and vapors through high-polymer films. xii. the permeability of gases and vapors through cellulose derivative films.* Kobunshi Kagaku, 1961. **18**: p. 124-132.

85. Ash, R., R.M. Barrer, and D.G. Palmer, *Solubility and transport of gases in nylon and polyethylene.* Polymer, 1970. **11**: p. 421-435.

86. Tikhomirov, B.P., et al., *Permeation, diffusion, and solution of gases and water vapor in unplasticized poly(vinylchloride).* Makromol. Chem., 1968. **118**: p. 177-188.

87. Stevenson, A. and G. Morgan, *Fracture of elastomers by gas decompression.* Rubber Chem. Technol., 1995. **68**: p. 197-211.

88. Gent, A.N. and D.A. Tompkins, *Nucleation and growth of gas bubbles in elastomers.* J. Appl. Phys., 1969. **40**: p. 2520-2525.

89. Stewart, C.W., *Nucleation and growth of bubbles in elastomers.* J. Polym. Sci. Part A-2, 1970. **8**: p. 937-955.

90. Jaravel, J., et al., *On key parameters influencing cavitation damage upon fast decompression in a hydrogen saturated elastomer.* Polym. Testing, 2011. **30**: p. 811-818.

91. Briscoe, B.J. and D. Liatsis, *Internal crack symmetry phenomena during gas-induced rupture of elastomers.* Rubber Chem. Technol., 1992. **65**: p. 350-373.

92. Briscoe, B.J. and S. Zakaria, *Gas-induced damage in elastomeric composites.* J. Mater. Sci., 1990. **25**: p. 3017-3023.

93. Briscoe, B.J. and S. Zakaria, *Sorption and dilation of silicone elastomer composites at high gas pressures: the role of interfacial quality.* J. Polym. Sci. Part B Polym. Phys., 1992. **30**: p. 959-969.

94. Briscoe, B.J. and S. Zakaria, *Interaction of CO2 gas with silicone elastomer at high ambient pressures.* J. Polym. Sci. Part B Polym. Phys., 1991. **29**: p. 989-999.

95. Major, Z. and R.W. Lang, *Characterization of the fracture behavior of NBR and FKM grade elastomers for oilfield applications.* Eng. Failure Anal., 2010. **17**: p. 701-711.

96. Shieh, Y.-T., et al., *Interaction of supercritical carbon dioxide with polymers. i. crystalline polymers.* J. Appl. Polym. Sci., 1996. **59**: p. 695-705.

97. Shieh, Y.-T., et al., *Interaction of supercritical carbon dioxide with polymers. ii. amorphous polymers.* J. Appl. Polym. Sci., 1996. **59**: p. 707-717.

98. Yamabe, J. and S. Nishimura, *Nanoscale fracture analysis by atomic force microscopy of EPDM rubber due to high-pressure hydrogen decompression.* J. Mater. Sci., 2011. **46**: p. 2300-2307.

99.   Yamabe, J., T. Matsumoto, and S. Nishimura, *Application of acoustic emission method to detection of internal fracture of sealing rubber material by high-pressure hydrogen decompression.* Polym. Testing, 2011. **30**: p. 76-85.

100.   Jaravel, J., et al., *Experimental real-time tracking and diffusion/mechanics numerical simulation of cavitation in gas-saturated elastomers.* Int. J. Solids Struct., 2013. **50**: p. 1314-1324.

101.   Tapeinos, I.G. and S. Koussios, *Experimental study on various liner materials for cryogenic liquid hydrogen storage.* Materials, 2013. **in press**.

102.   Theiler, G. and T. Gradt, *Polymer composites for tribological applications in hydrogen environment.* Proceedings of the 2nd International Conference on Hydrogen Safety, 2007.

103.   Zhang, Z., et al., *Sliding performance of polymer composites in liquid hydrogen and liquid nitrogen.* J. Mater. Sci., 2004. **39**: p. 2989-2995.

DISTRIBUTION

1   MS0899   Technical Library   9536 (electronic copy)